International Atomic Energy Agency

INDC(CCP)-335
Distr.: L

INDC INTERNATIONAL NUCLEAR DATA COMMITTEE

*TRANSLATION OF SELECTED PAPERS*

PUBLISHED IN YADERNYE KONSTANTY (NUCLEAR CONSTANTS 3, 1990)

(Original Report in Russian was distributed
as INDC(CCP)-328/G)

Translated by A. Lorenz
for the
International Atomic Energy Agency

July 1991

IAEA NUCLEAR DATA SECTION, WAGRAMERSTRASSE 5, A-1400 VIENNA

INDC(CCP)-335
Distr.: L

# TRANSLATION OF SELECTED PAPERS
# PUBLISHED IN YADERNYE KONSTANTY (NUCLEAR CONSTANTS 3, 1990)

(Original Report in Russian was distributed
as INDC(CCP)-328/G)

Translated by A. Lorenz
for the
International Atomic Energy Agency

July 1991

Reproduced by the IAEA in Austria
August 1991

91-03116

Contents

# THE TOTAL NEUTRON CROSS-SECTION AND RESONANCE PARAMETERS FOR THE EVEN $^{58,60,62,64}$Ni ISOTOPES FOR ENERGIES RANGING FROM 2eV TO 8000eV

L.L. Litvinskij, P.N. Vorona, V.G. Krivenko, V.A. Libman,
A.V. Murzin, G.N. Novosselov, N.A. Trofimova,
O.L. Tchervonnaya
Institute of Nuclear Research of the Ukranian SSR, Kiev

Abstract

The total cross-sections of the $^{58,60,62,64}$Ni isotopes were measured in the 2 eV to 8000 eV energy region by the time-of-flight method at the WWR-M nuclear reactor of the Institute of Nuclear Research of the UkSSR AS. The potential scattering radii and the nearest positive resonance parameters were also determined.

Microscopic neutron data of the isotopes of nickel, which plays an important part in the composition of structural materials, are of particular interest in a number of applied neutron-physical problems, such as in the calculations of both thermal and fast nuclear reactors, in the development of fusion reactors, in nuclear geophysics applications, etc. In a number of applications, there are particular needs for nickel isotope neutron cross-sections at energies ranging up to a few tens of kilo-electronvolts.

In the course of the last few years, most of the evaluated nickel isotope neutron cross-section data files in the ENDF, JENDL, BNAB and other evaluated data libraries, have been re-evaluated. At the same time, there is a remarkable lack of reliable experimental data on the total cross-section $\sigma_t$ of these nuclides in the $E_n$ < 10 keV energy range [1].

In addition to the importance which experimental data have in the solution of applied problems, information on the total cross-sections of A≈60 nuclides bears upon the systematics of neutron

resonances and on the choice of formalisms in the evaluation of neutron cross-sections in the range of isolated resonances. As an example, the applicability of the simplest multilevel formulae to the description of neutron cross-sections in the region of minima [2], is still an open question.

Dependable experimental total neutron cross-section data for nuclides in the A≈60 region, in the few tens of keV energy range, are also needed for the development of neutron interference filters based on stable isotopes [3].

In response to these requirements, the total neutron cross-sections of the even isotopes of nickel were measured in the energy rang of $E_n$=2-8000 eV, at the WWR-M nuclear reactor of the Institute of Nuclear Research (INR) of the UkSSR Academy of Sciences (AS UkSSR), using a mechanical energy selector and the time-of-flight method. In addition, the potential scattering radii $R_0'$ of the partial neutron s-wave, the local values of the average radiation widths $\overline{\Gamma}_\gamma$ for the energy $E_\lambda$ and the neutron width $\overline{\Gamma_{n_\gamma}}$ of both negative and positive nearest lying resonances for the $^{58,60,62,64}$Ni isotopes were derived from the analysis of the experimental data.

## Experimental Technique

The total neutron cross-section $\sigma_t$ was measured by the transmission method using the neutron spectrometer positioned on the horizontal channel of the WWR-M reactor of the AS UkSSR INR. The length of the neutron pulse, determined by a mechanical pulse selector, was 5 μs. The neutrons were counted at a flight distance of ≈70 m with a battery of $He^3$ detectors. The description of the experimental setup and of the schematics of the electronics are described in references [4] and [5].

In order to reduce the gamma background and background generated by the multiple scattering of fast neutrons, the neutron beam was filtered by a ≈25 g/cm$^2$ thick metallic filter of nickel-60, located immediately behind the mechanical velocity selector The transmission of gamma rays having average energies of 2-3 MeV

TABLE 1. COMPOSITION OF $^{58,60,62,64}Ni$ SAMPLES

| Isotope | Sample Number | Thickness | Isotopic composition % | | | | |
|---|---|---|---|---|---|---|---|
| | | | $^{58}Ni$ | $^{60}Ni$ | $^{61}Ni$ | $^{62}Ni$ | $^{64}Ni$ |
| $^{58}Ni$ | 1 | 8.22(1) | 99.75(12) | 0.16(1) | 0.010(1) | 0.040(5) | 0.045(5) |
| $^{60}Ni$ | 1 | 157.9(2) | 0.67(6) | 99.22(10) | 0.060(6) | 0.040(4) | 0.010(1) |
| | 2 | 93.1(1) | 0.76(7) | 99.13(10) | 0.060(6) | 0.040(4) | 0.010(1) |
| | 3 | 51.71(5) | 1.19(12) | 98.69(10) | 0.070(7) | 0.040(4) | 0.010(1) |
| $^{62}Ni$ | 1 | 4.351(4) | 0.62(6) | 1.01(10) | 0.26(3) | 98.04(10) | 0.070(7) |
| $^{62}Ni$ | 2 | 0.4251(4) | - | - | - | - | - |
| $^{64}Ni$ | 1 | 3.769(4) | 4.14(42) | 2.49(25) | 0.22(3) | 1.25(13) | 91.9(1) |

through the filter was $T_\gamma \approx 0.3$, and the transmission of neutrons with energies larger than 10 keV was $T_n \leq 0.1$. In the region of the first interfering minimum of nickel-60 (at E=1-8000 eV), the neutron transmission was $T_n \geq 0.8$. The use of the nickel-60 filter made it possible to reduce the need for the correction of the background correlated to the neutron beam (i.e., the background created by multiple scattering of neutrons in the structural elements surrounding the detectors.

The metallic samples used in these measurements were highly enriched (92-99%) in the isotope which was measured. The sample characteristics are given in Table 1. Corrections for the contamination of the even isotopes of nickel were calculated by the method of successive approximation based on data obtained in this experiment. Evaluated data from the JENDL-2 [6] evaluated data library were used to correct for the odd nickel isotope $^{61}Ni$.

## Parametrization of neutron cross-sections

In the energy range of E=2-8000 eV, the resonance Doppler broadening quantity $\Delta$ for the nickel isotopes is equal to:

$$\Delta = 2\sqrt{\frac{2k_B \cdot T^{\circ} E}{A+1}} \leq 2\,eV \qquad (1)$$

as the s-resonance widths of the even nickel isotopes are equal to $\Gamma_n \approx 1$ keV $\gg \Delta$, and the contribution from the p-resonances in this energy range is insignificant, Doppler broadening of the experimental data was not taken into consideration.

In the parametrization of the experimental data, the total neutron cross-section was expressed in terms of collision matrix elements $S_{nn}^{J\pi}$ :

$$\sigma_t(E) = \frac{2\pi}{k^2} \sum_{J\pi} g(J) \sum_{sl} \left[1 - ReS_{nn}^{J\pi}\right] \qquad (2)$$

where J and $\pi$ are the spin and parity of the combined system, S is the spin of the channel, l the orbital moment of the neutron, and $g(J)=(2J+1)/2(2I+1)$ is the statistical spin factor.

The diagonal elements of the collision matrix $S_{nn}^{J\pi}$ were determined in a multi-level R-matrix approximation [2] using elements of the R-matrix $R^{J\pi}$ and phases of the potential scattering function $\varphi^l$ :

$$S_{nn}^{J\pi} = e^{-2i\varphi_l} \cdot \frac{1 + iR^{J\pi}}{1 - 1R^{J\pi}} \qquad (3)$$

The $R^{J\pi}$ elements were defined as:

$$R^{J\pi}(E) = \frac{1}{2} \sum_{\lambda(J\pi)} \frac{\Gamma_{n\lambda}}{E_\lambda - E - (i\overline{\Gamma}_\gamma)/2} \qquad (4)$$

where $E^\lambda$ and $\Gamma^{n\lambda}$ represent the energy and neutron width $\lambda$ of the resonance, $\overline{\Gamma^\gamma}$ the average radiation width of the resonances in the energy interval being investigated. The energy dependence of the neutron widths was based on the relationship:

$$\Gamma_{n\lambda} = \sqrt{E} \cdot v_l \cdot \Gamma_{n\lambda}^{o} \qquad (5)$$

where $\Gamma_{n\lambda}^{0}$ is the energy independent neutron width, and $v_l$ is the optical transmission factor.

The potential scattering phases for the s- and p- partial neutron waves were defined by:

$$\varphi_0 = ka - \arctan(kaR_0^{\bullet})$$

$$\varphi_1 = ka - \arctan(ka) - \arctan\left[\frac{(ka)^3 R_0^{\bullet}}{1 + (ka)^2 + R_1^{\bullet}}\right] \qquad (6)$$

where $a=1.35\cdot A^{1/3}$ fermi; $R_0^{\bullet}$ and $R_1^{\bullet}$ are the potential scattering parameters for the s- and p-waves. The quantity $R_0^{\bullet}$ was derived from the potential scattering radius R′ using the equation

$$R_0^{\bullet} = 1 - \frac{R'}{a} \qquad (7)$$

Equations (2) to (7) were used in the parametrization of experimental total neutron cross-section data by means of the least squares method for various set of varying parameters, i.e., R′, $\bar{\Gamma}_\gamma$, $E_\lambda$ and $\Gamma_{n\lambda}$.

## Discussion of the Results

a) Nickel-58

The results of the measured total neutron cross-section $\sigma_t$ of nickel-58 in the energy range 2 to 8000 eV are shown in Fig. 1 together with the more recent evaluation given in JENDL-2 [6], represented by the dotted curve. The values for $\sigma_t$ measured in this experiment in the energy range E=2-1000 eV are systematically 5% lower than the evaluation given in reference [6]. In the energy range of 1000 to 5000 eV, the results of this experiment agree with the JENDL-2 values within the limits of the experimental error, and in the E=5000-8000 eV energy range, our results fall 10%-30% above those of reference [6].

The contribution of two negative and twenty-two positive neutron resonances were taken into account in the analysis of the nickel-58 experimental data (all s- and p-resonances were included in the analysis up to the neutron energy of 63 keV, and in the 63<E<205 keV energy range only the contribution of s-resonances were taken into account). Values of the fixed resonance parameters were taken from the reference [6] evaluation. The analysis showed that there is only a slight dependence on the

TABLE 2. RESULTS OF THE NICKEL-58 $\sigma_t$ ANALYSIS

| R′ (Fermi) | $\Gamma_{n-1}$ keV $E_{-1}$=5.50 keV [6] | $\Gamma_{n-2}$ keV $E_{-2}$=28.8 keV [6] | Reference |
|---|---|---|---|
| 8.7±1.2 | 0.585±0.075 | 7.0±2.0 | This work |
| 8.087 | 1.06 | 7.87 | JENDL-2 [6] |
| 8.0±0.5 | - | 15.5±0.8 | BNL-325 [7] |

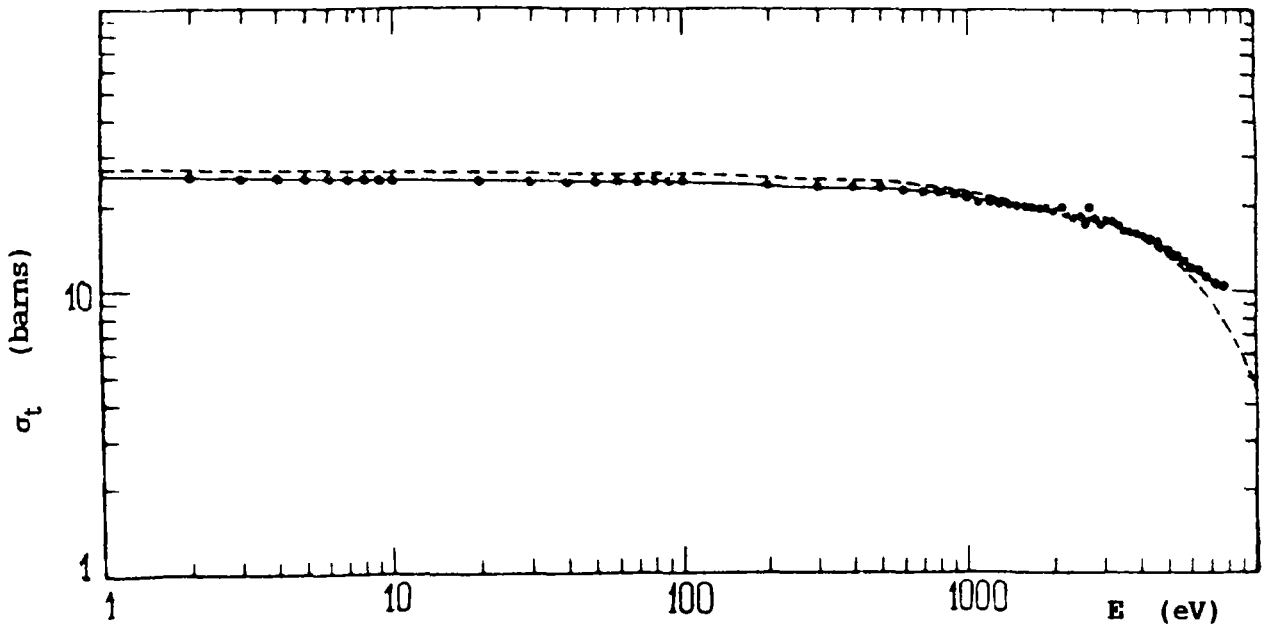


Fig. 1. Total neutron cross-section of nickel-58

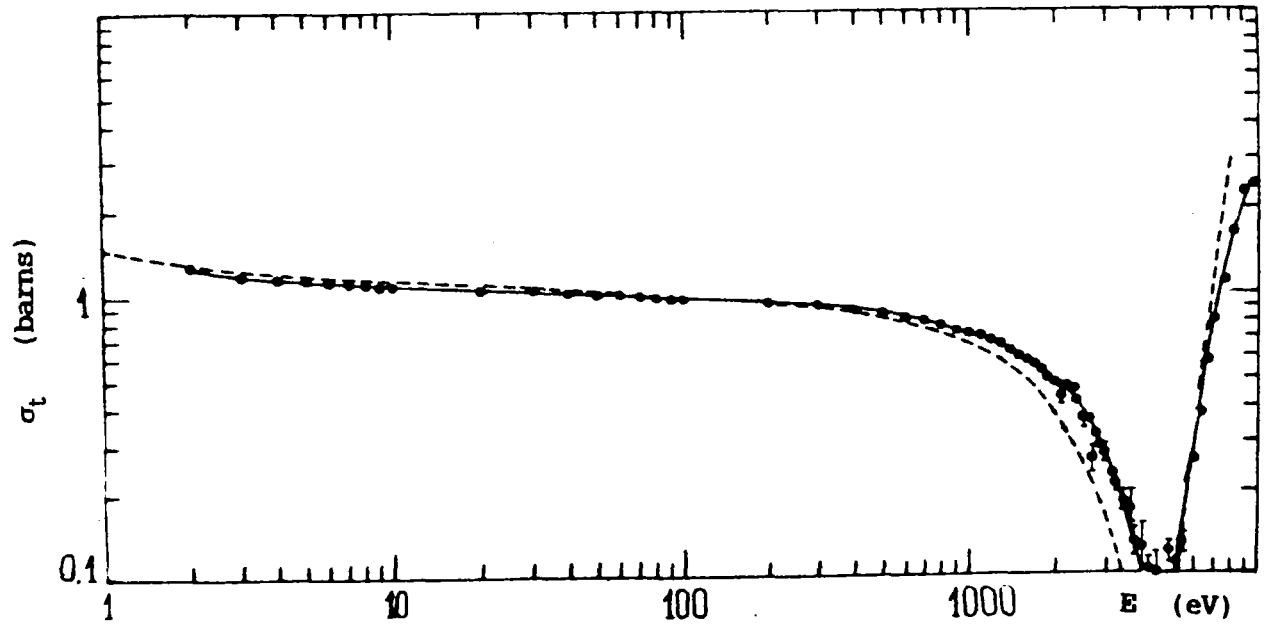


Fig. 2. Total neutron cross-section of nickel-60

average radiation width $\bar{\Gamma}_\gamma$ and on the parameters of the nearest positive s-resonance which lies outside of the analyzed energy range of 2 to 8000 eV. The basic parameters which were determined to a high enough accuracy from the measured values of the total cross-section of nickel-58 are the potential scattering radius R' and the neutron width of the negative resonances $\Gamma_{n-1}$ and $\Gamma_{n-2}$ (see TABLE 2). The result of the approximation of the experimental data are represented in Fig. 1 by the continuous curve.

Within the limits of its uncertainty, the value obtained for R' agrees well with the evaluations given in references [6] and [7]. The value for $\Gamma_{n-2}$ agrees well with the more recent JENDL-2 evaluation, but the value for $\Gamma_{n-1}$ obtained in this experiment is approximately twice as large as the value given in reference [6]. Since there havn't been any reliable experimental data on $\sigma_t$ for nickel-58 prior to this experiment, particularly in an energy range which is susceptible to the inclusion of negative resonances, it can be said that the values for $\Gamma_{n-1}$ and $\Gamma_{n-2}$ derived from this experiment can be considered to be reliable.

Information on negative resonances for $E_{-1}$=-5.5 keV are absent in the BNL-325 [7] compilation. According to the data given in the JENDL-2 [6] evaluated data library, this particular resonance has a rather large neutron width of $\Gamma_{n-1}$ = 1.06 keV. This led us to the question whether it is reasonable to include the contribution of the two negative resonances in the evaluation of the measured total cross-section data. Our analysis showed that the consideration of one "effective" negative resonance instead of two did not worsen the approximation of the experimental data. However, the value of R'≈10.5 f obtained on this assumption, is significantly different from the value of R'≈8.0 f given in references [6] and [7], which were derived from an analysis of experimental data over a broad energy range. Since there is no basis for a strong local fluctuation of R', it is necessary to recognize the presence of at least two strong negative resonances in the proximity of the binding energy.

b) Nickel-60

A comparison of the measured values of the total cross-section of nickel-60 (shown by individual points) obtained in this experiment with evaluated results given in the evaluated data library JENDL-2 [6] (shown as a dotted curve) is given in Fig. 2. In the energy range of 1 t0 100 eV, the total cross-section values obtained in this experiment are lower than the JENDL-2 values [6] by ≈5%. A considerable difference (of ≥50%) between the results of this measurement and those of the JENDL-2 [6] evaluation can be seen in the region of the interfering minimum at E=1000-8000 eV.

The contribution of the nearest negative resonance and of the eleven positive resonances (i.e., all known s- and p-resonances up to the energy of 43 keV) were considered in the analysis of the experimental data. All fixed resonance parameters were taken from the evaluated data library JENDL-2 [6].

The analysis has shown that the experimental data cannot be described satisfactorily without taking the variations of the negative resonance parameters into consideration. In order to adequately approximate the measured values of the total cross-section it was found to be necessary to reduce considerably (i.e., by more than a factor of 10) the contribution of the negative resonance to the total cross-section so as to arrive at values comparable to those given in references [6] and [7]. Further calculations showed that the approximation of the experimental data with no consideration given to the negative resonance, does not make the approximation any worse than if its contribution is included in the approximation. The values of the total cross-sections for nickel-60 which have been obtained in this experiment can be considered to be reliable, particularly in the energy range of E<8000 eV where they are especially susceptible to the effects of negative resonance parameters. Therefore, the inclusion of the negative resonance in the evaluation of the nickel-60 neutron cross-section does not appear to be sensible.

Final results of the analysis are given in Table 3. The result of the approximation of the experimental data is shown in Fig. 2 by the plain curve.

TABLE 3. RESULTS OF THE NICKEL-60 $\sigma_t$ ANALYSIS

| $\bar{\Gamma}_g$ (eV) | R' (fermi) | $E_1$ (keV) | $\Gamma_{n1}$ keV | References |
|---|---|---|---|---|
| 4.26±0.17 | 7.21±0.15 | 12.34±0.20 | 7±0.090 | This work |
| 1.9 | 6.98 | 12.46 | 2.353 | JENDL-2 [6] |
| 1.7 | 6.7±0.3 | 12.500 | 2.7±0.1 | BNL-325 [7] |

The values for the potential scattering radius R', the energy $E_1$ and the neutron width $\Gamma_{n1}$ of the first positive s-resonance agree very well with the data given in references [6] and [7].

In the analyzed energy region of 2-8000 eV, which corresponds to the interfering minimum of the first s-resonance, the local value of the average radiation width $\bar{\Gamma}_\gamma$ is practically the same as that of the radiation width $\bar{\Gamma}_{\gamma 1}$ of this resonance. The value of these quantities, namely $\bar{\Gamma}_\gamma \approx \Gamma_{\gamma 1} = 4.3 \pm 0.1$ eV, is significantly different from the evaluated values of the average radiation width (see Table 4) and of the radiation width of the closest s-resonance $\Gamma_{\gamma 1}$, given in reference [6] as 2.73 eV, and as 3.3±0.3 eV in reference [7]. The values of $\Gamma_{\gamma 1}$ given in references [6,7] were derived from an analysis of the radiation capture cross-section $\sigma_\gamma$ because data for $\sigma_t$ in the range of the interfering minimum, which has a strong effect on the value of $\Gamma_{\gamma 1}$, were not available before the performance of this experiment. The $\sigma_\gamma$ data yield reliable information on the ratio of the widths $\Gamma_\gamma/\Gamma_n$. The value of the neutron width $\Gamma_{n1}$=2.7±0.1 keV evaluated in reference [7] exceeds the value given in reference [6] as well as the value of 2.35 keV derived in this work. A correction applied to the data given in reference [7] yields a value of $\Gamma_{\gamma\gamma} = 3.8 \pm 0.3$ eV which is in agreement with the data obtained in this experiment within the limit of its uncertainty.

c) Nickel-62

Fig. 3 shows a comparison of the measured total cross-section values for nickel-62 (individual points) with the evaluated data given in reference [6] (shown by the dotted line). The data of this experiment lies ≈20% below the evaluated data given in JENDL-2 [6] over the entire 2-8000 eV energy range.

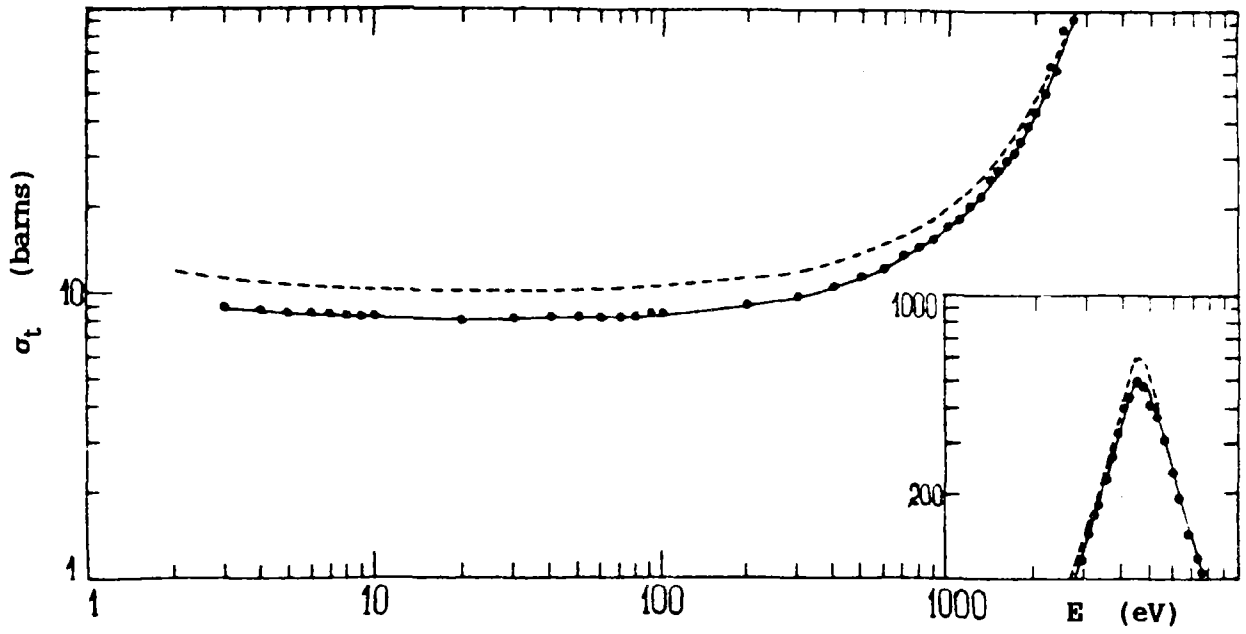


**Fig. 3. Total neutron cross-section of nickel-62**

The following parameters for the negative resonance of nickel-62 are listed in reference [7]: $E_{-1}$=-0.077 keV, and $\Gamma_{n-1}$=0.14 keV. The more recent experimental data evaluation published in JENDL-2 [6] does not take the contribution of the negative resonance into account in the derivation of the evaluated cross-sections. The values of $\sigma_t$ obtained in the analysis of this experiment confirms the conclusions of reference [6], by showing that a satisfactory description of the experimental data does not necessitate the inclusion of the negative resonance in this analysis.

The evaluation of the experimental nickel-62 total cross-section included the contribution of 24 known positive s- and p-resonances with energies <106 keV. Values of the fixed resonance parameters were taken from reference [6]. The results of this evaluation are listed in Table 4, and the curve approximating the experimental data is shown by the continuous line in Fig.3.

TABLE 4. RESULTS OF THE NICKEL-62 $\sigma_t$ ANALYSIS

| $\bar{\Gamma}_\gamma$ (eV) | R' (fermi) | $E_1$ (keV) | $\Gamma_{n1}$ (keV) | Reference |
|---|---|---|---|---|
| 3.09±0.25 | 7.80±0.14 | 4.607±0.018 | 1.822±0.018 | This work |
| 1.3 | 7.64 | 4.600 | 2.026 | JENDL-2 [6] |
| 0.91 | 6.2±0.3 | 4.54±0.05 | 1.88±0.20 | BNL-325 [7] |

The value of R' obtained in this analysis does not agree with the data given in reference [7], but it confirms the results given in reference [6]. The parameters for the first s-resonance $E_1$, $\Gamma_{n1}$ obtained in this analysis agree with the data given in references [6] and [7] if one exceeds the limits of their uncertainties.

In the given energy range, the local value of the average radiation width $\bar{\Gamma}_\gamma$ is basically determined by the radiation width $\Gamma_{n1}$ of the strong s-resonance which falls in this energy range. The value $\bar{\Gamma}_\gamma$=3.09±0.25 eV which was obtained is significantly different than the data given in references [6] and [7] for the average radiation width (see Table 4) and for the radiation width of the first s-resonance: $\Gamma_{\gamma 1}$=0.76±0.12 eV. There is a slightly better agreement with the value $\Gamma_{\gamma 1}$=2.38 eV given in reference [6]. The correction of the $\Gamma_{n1}$ value in accordance with the procedure described above, yields a value of 2.7 eV for $\Gamma_{\gamma 1}$, which falls within the limits of the uncertainty of this work.

d) Nickel-64

Fig. 4 shows a comparison of the total nickel-64 cross-section values obtained in this experiment (represented by individual points) with the data published in reference [6] (represented by the dotted curve). The results based on this experiment are in good agreement with the evaluated $\sigma_t$ data given in reference [6].

The analysis of the experimental data took into account the contribution of 24 known s- and p-resonances with energies below 310 keV. Fixed resonance parameters were taken from the evaluated data given in reference [6]. The results of this evaluation are shown in Table 5 and Fig.4 (represented by the continuous curve). Within the limits of the uncertainties, the results obtained for R' and $\Gamma_{n1}$ are in good agreement with the data published in references [6] and [7].

TABLE 5. RESULTS OF THE NICKEL-64 $\sigma_t$ ANALYSIS

| R' (fermi) | $\Gamma_{n1}$ (keV) $E_1$=14.3 keV [6,7] | Reference |
|---|---|---|
| 7.4±1.0 | 2.9±0.2 | This work |
| 7.36 | 2.900 | JENDL-2 [6] |
| 7.6±0.3 | 2.90±0.50 | BNL-325 [7] |

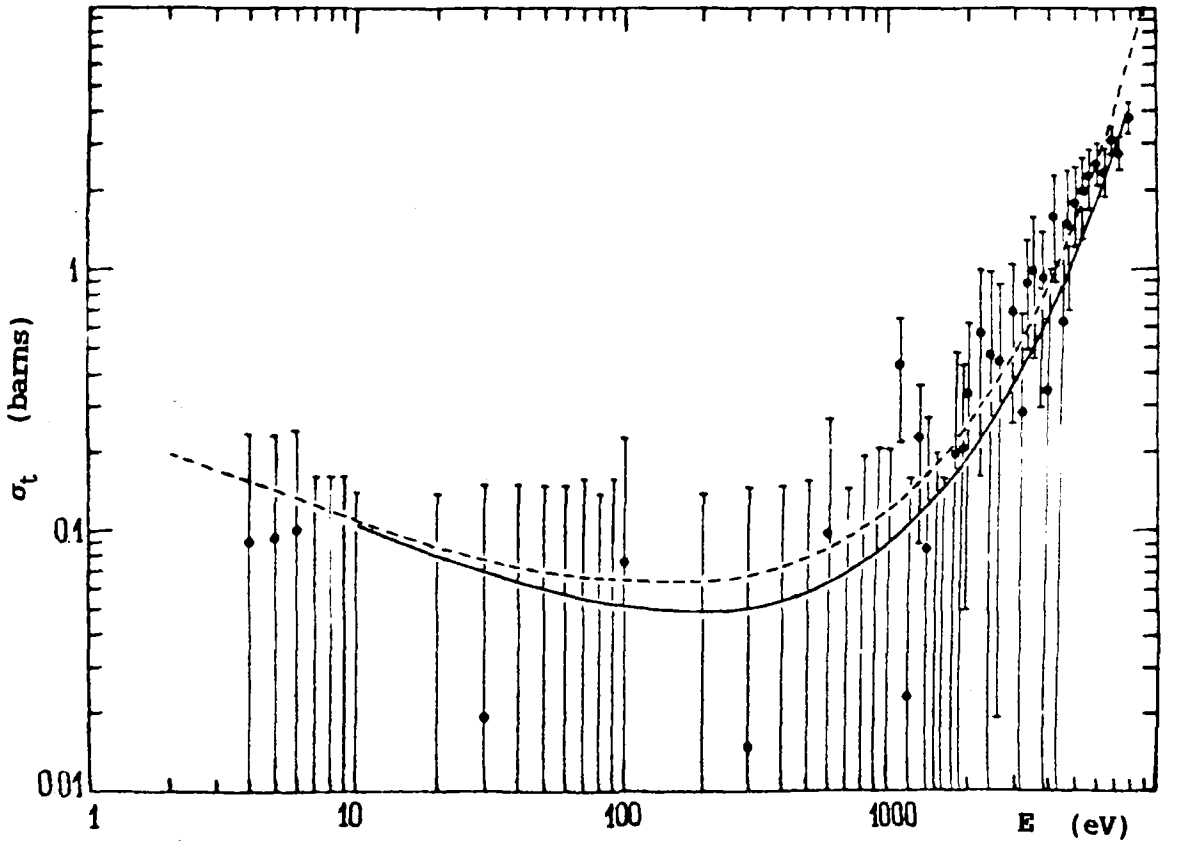


**Fig. 4. Total neutron cross-section of nickel-64**

e) The isotopic dependence of the potential scattering radius of even isotopes of nickel.

Figure 5a shows a comparison of the s-wave potential scattering radii R' for the even isotopes of nickel derived in this experiment with the evaluated data given in references [6] and [7]. The R' data values obtained in this evaluation agree with those of reference [6]. The evaluated data given in reference [6] and those derived in this experiment are also in good agreement with the prediction of the generalized optical model of a weak floating dependence of R' on the mass number A as one moves away from the double magic number of $^{56}$Ni (see the solid curve, Fig.5a). However, the minimum of the R'(A) dependence (see dashed curve) which agrees with the data of reference [7] at A=62, is not confirmed by our results. The absence of any irregularity in the evaluated data given in reference [7] for A=62 (e.g. for the average distance between s-resonances $\bar{D}$ shown in Fig. 5b, and for the s-neutron strength function $S_0$ shown in

Fig. 5c) is yet another argument in favor of a floating dependence of R′ on the mass number A, which has been observed in the results of this experiment.

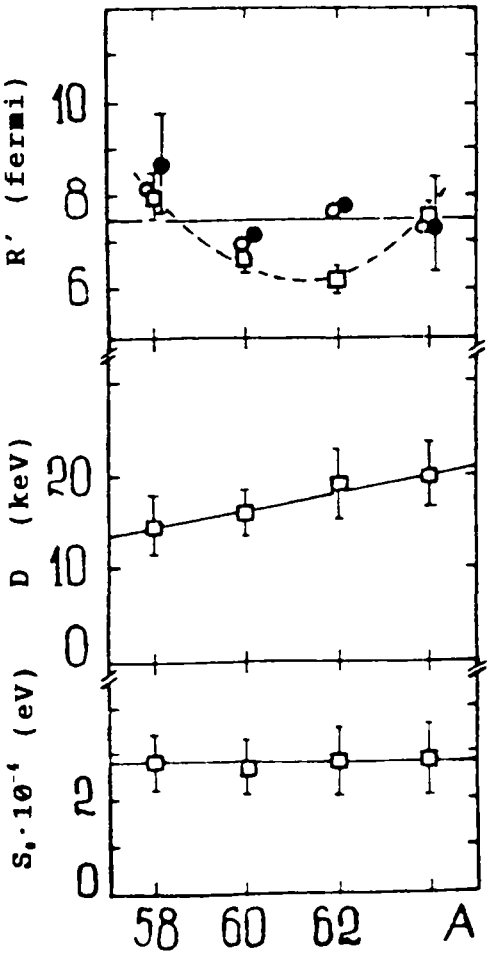


Fig. 5. Dependence of the potential scattering radius (5a), of the average distance between levels (5b), and the s-strength function (5c), on the mass number of even isotopes of nickel:
∘ - data from reference [6],
□ - data from reference [7],
● - data from this experiment.

## Conclusion

The analysis of new experimental data on the total neutron cross-section $\sigma_t$ of even isotopes of nickel in the energy range of 2 eV to 8000 eV has demonstrated the possibility to substantiate the evaluation of the total cross-section using simple multilevel expressions which are valid near interfering minima of strong s-resonances (nickel-60 and 64), in the proximity of the actual resonances (nickel-62) as well as far removed from strong resonances (nickel-58). In the given energy range, the experimental data has exhibited a strong sensitivity to parameters of negative resonances, and in the neighborhood of interfering minima (nickel-60,64) the data are strongly dependent on the potential scattering radius R′ and on all parameters of the nearest lying resonance, namely $E_\lambda$, $\Gamma_{\gamma\lambda}$ and $\Gamma_{n\lambda}$.

## REFERENCES


[1] MCLANE, V., Neutron Cross-Sections, Academic Press, Vol. 2 (1988).

[2] LUK'YANOV, A.A., The Structure of Neutron Cross-Sections, Atomizdat, Moscow (1978) (in Russian).

[3] MURZIN, A.V., VERTEBNYIJ, V.P., GAVRILYUK, V.I., At.Ehnerg. 3 (1989) 216-218 (in Russian).

[4] VERTEBNYIJ, V.P., VORONA, P.N., KAL'TCHENKO, A.I., Neutron Physics, Part 2, Naukova Dumka, Kiev (1972) (in Russian).

[5] OFENGENDEN, R.G., BEREZIN, F.N., VASSILENKO, N.P., et al., Neutron Physics, Vol. 4, TsNIIIAtominform, Moscow (1988) (in Russian).

[6] KIKUCHI, Y., SECINE, N., Evaluation of Neutron Nuclear Data of Natural Nickel Isotopes for JENDL-2, Rep. JAERI-M-85-101 (1985) 1-96.

[7] MUGHABGHAB, S.F., Neutron Cross-Sections, Rep. BNL-325, Vol.1 (1984).

# THE $^{54}Fe(n,\alpha)^{51}Cr$ THERMAL NEUTRON REACTION CROSS-SECTION

S.P. Makarov, G.A. Pik-Pitchak, Yu.F. Rodionov,
V.V Khmyzov, Yu.A. Yashin
I.V. Kurchatov Institute of Atomic Energy, Moscow

Abstract

Measurement and theoretical evaluation of the thermal neutron induced $^{54}Fe(n,\alpha)^{51}Cr$ reaction cross-section are described. The following parameters of this reaction were determined: $\langle\sigma_\alpha\rangle_{calc} \approx 1.1\times10^{-27}$ barns, RI ≈ 0.6 mbarns, $(\sigma_\alpha)_{exp} \approx 1\times10^{-5}$ barns, RI ≈ 1.09±0.13 mbarns.

The thermal neutron induced $^{54}Fe(n,\alpha)^{51}Cr$ reaction cross-section, which has a thermal cross-section of $\sigma_\alpha$=(0.37±0.001) barns [1], is used in calculations [2,3] to investigate the migration of radionuclides which originate in the first cooling loop of nuclear power plants as a result of corrosion. This reaction also has a significant contribution to the activation of $^{54}Fe$ which is a component of reactor structural materials. The investigation of this reaction by many authors [4,5,6,7,8] suggests the ambiguous nature of the data on this reaction.

Due to the importance which the process of $^{51}Cr$ production has in the operation of nuclear power reactors, and based on our suspicion that the value of $\sigma_\alpha$, which is given above, to be too high as well as dubious (in view of the low uncertainty of ±0.3% given to the result published in reference [1]), it was decided to perform a theoretical analysis as well as a measurement of this reaction.

The $(n,\alpha)$ reaction, which proceeds through the formation of a compound nucleus, is evaluated with the aid of the statistical model [9,10,11,12,13] which assumes that the neutron is captured with a zero angular momentum, and that the $\alpha$-particle is emitted with an arbitrary moment equal to $\hbar l$:

$$\sigma_\alpha = \pi R_n^2 \Gamma_\alpha / (\Gamma_n + \Gamma_\gamma + \Gamma_\alpha)$$

*where* $R_n = [\, r_o (A-1)^{1/3} + 1.4 \,]$ *fermi*, $\Gamma_\gamma = 4.0 \cdot 10_{-8}$ *MeV*

$$\Gamma_n = (\pi D_n)^{-1} \int_o^{E_n - Q_n} \varepsilon \, d\varepsilon \rho_n (E_n - Q_n - \varepsilon) / \rho_c (E)$$

$$\Gamma_\alpha = [2\pi \rho_c (E)] \int_o^{E_\alpha - Q_\alpha} \rho_\alpha (E_\alpha - Q_\alpha - \varepsilon_\alpha) \sum_{l=o}^{\infty} (2l+1)^2 T_l (\varepsilon_\alpha) \, d\varepsilon_\alpha$$

$$E = Q + \varepsilon_n^o + \Delta, \quad E_n = Q_n + \varepsilon_n^o + \Delta_n, \quad E_\alpha = Q_n + \varepsilon_\alpha^o + \Delta_\alpha$$

where $\Delta = \Delta_\alpha = 1.8$ MeV, $\Delta_n = 3.6$ MeV, $Q_n = 9.30$ MeV and $Q_\alpha = 8.456$ MeV and $\varepsilon_n^0$ is the neutron capture kinetic energy. The level density of the compound nucleus is represented by:

$$\rho_l (E_l) = const \cdot (\delta + E_l^2)^{-1} \exp (2\sqrt{a_l E_l})$$

*where* $a_l = A_l / 10$, $D_l = h^2 (2mR_l^2)^{-1}$, $\delta = 1.0 MeV$

For the $\alpha$-particle energy in the sub-barrier region, we have:

$$T_1 (\varepsilon) = \exp (-2\gamma_1 (\varepsilon)) \ ,$$

$$\gamma_1 (\varepsilon) = \frac{b}{2\sqrt{f}} \left[ \frac{\pi}{2} + A - B + C \right]$$

*where* $$A = \arctan \frac{b-2f}{2\sqrt{f}\sqrt{b+c+f}}$$

$$B = \sqrt{b+c+f}$$

$$C = \sqrt{c} \ln \left[ \frac{2\sqrt{c(c+b-f)} + 2c + b}{\sqrt{b^2 + 4cf}} \right]$$

*and where* $c = l(l+1)$, $b = B_\alpha / D_\alpha$, $f = \varepsilon / D_\alpha$, $B_\alpha = 2(z-2)\, e^2 / R_\alpha$

For thermal neutrons, we obtained a value of $\sigma_{\alpha}=1.1\times10^{-27}$. For $^{235}U+n$ or $^{239}Pu+n$ fission spectrum neutrons we obtained the Maxwellian spectrum averaged values of $T_{eff}=1.318$ MeV and $\langle\sigma_{\alpha}\rangle=0.6\times10^{-3}$ barns.

The experimentally determined value of the $(n,\alpha)$ reaction cross-section at thermal was obtained by measuring the content of the $^{51}Cr$ isotope in the irradiated iron sample. The experiment was conducted on the uranium-graphite reactor F-1 of the I.V. Kurchatov Institute of Atomic Energy (IAE). The irradiated sample consisted of $Fe_2O_3$ in powder form enriched in $^{54}Fe$ to 90.7%, enclosed in a cylindrically shaped aluminum container; the total mass of $^{54}Fe$ was 11.74 g.

The analysis, which was performed at the central analytical laboratory of the IAE, used atomic emission spectrometry and a high-frequency induction plasma source for spectrum excitation to determine the composition of the original sample; the result of this analysis showed that the concentration of chrome in the original sample was smaller than $1.7\times10^{-3}$%, that is, chrome was not detected. The content of radionuclides in the sample, both prior to and after irradiation was determined from the intensity of their gamma ray emission. A calibrated gamma ray spectrometer and detector made of high purity germanium [14], used in this experiment had an energy resolution of 1.5 keV for 320 keV gamma rays. The chrome-51 in the sample was identified by its 320.1 keV gamma ray and its half-life of 27.73 days.

The first irradiation was performed in the calibrated thermal column of the F-1 reactor with a thermal neutron flux of $(1.66\pm0.03)\times10^{11}$ $n/m^2$ s, for an irradiation exposure of 100 days. The equilibrium activity level of the $^{51}Cr$ in the sample was attained with due consideration given to the reactor operating history and the decay of this radionuclide between irradiations. For a value of $\sigma_{\alpha}=0.37$ barns, the equilibrium activity of $^{51}Cr$ was calculated to have reached a level of $1.5\times10^{4}$ Bq. The total 320.1 keV absorption peak was not detected in the measured spectrum of gamma ray emitted by the sample. In our case, the level of reliability to detect this gamma line of $^{51}Cr$ was 1Bq.

This result was used to determine the upper limit of the investigated cross-section to be $\sigma_\alpha < 2.5 \times 10^{-5}$ barns.

The following well-known formula was used to calculate the activity and cross-section of $^{51}Cr$:

$$\lambda N_{51} = \sigma_\alpha \Phi_T N_{o54} [1 - \exp(-\lambda_{51} t_{irr})] + \lambda N_{o51} \exp(-\lambda_{51} t_{irr})$$

where $\lambda N_{51}$ is the $^{51}Cr$ activity at the end of irradiation,
$\lambda = 2.89 \times 10^{-7}$ $s^{-1}$ is the decay constant of $^{51}Cr$,
$N_{51}$ is the number of $^{51}Cr$ atoms, and
$N_{54}$ is the number of $^{54}Fe$ atoms.

As we were not able to detect any $^{51}Cr$ in the first run of this experiment, we decided to perform a second irradiation run in the horizontal channel of the same reactor which has a thermal neutron flux of $\Phi_T = 6.06 \times 10^{13}$ $n/m^2 \cdot s$. According to the calibration data of this reactor channel, the additional contribution of resonance neutrons was ≈6%. Two separate three-hour irradiation runs were made: one in which the sample was wrapped in cadmium foil and the other without cadmium shielding. In both instances, $^{51}Cr$ as well as $^{54}Mn$, $^{59}Fe$, and $^{197}W$, were identified in the gamma ray analysis of the irradiated iron oxide sample. The activity of the $^{51}Cr$ was (160±16) Bq and (165±16) Bq for the two runs, respectively. Since the results of both irradiation runs overlap within the limits of their uncertainties, it could be inferred that the $^{54}Fe(n,\alpha)^{51}Cr$ reaction is reactive to resonance neutrons. However, if one assumed that the value of the uncertainty of the different measured activities is due to the fact that the reaction is a thermal neutron reaction, then one could deduce from the following inequality:

$$m_{Fe^{54}} \cdot \frac{6.03 \times 10^{23}}{54} \sigma_\alpha \Phi_T [1 - \exp(-\lambda_{51} t_{irr})] < 22.6 Bq$$

that $\sigma_\alpha < 1 \times 10^{-5}$ barns. This experimental result does not contradict the theoretically evaluated value of $\sigma_\alpha$ derived above.

On the other hand, if one assumed that the chrome production was due exclusively to the thermal neutron $^{50}Cr(n,\gamma)^{51}Cr$ reaction, which has a cross-section of 15.9±0.2 barns [15], then, taking

into account that the natural abundance of $^{50}Cr$ isotope in elemental iron is 4.31%, then one obtains the result that the admixture of chrome in the investigated sample of iron oxide is less than $8.6 \times 10^{-4}$%. This result agrees with the evaluated chrome concentration obtained by the atomic emission spectrometric method.

On the basis of the derived value of the chrome activity $A_{Cr51}=(165\pm16)$ Bq, and a calibrated F-1 reactor neutron flux intensity relationship of $\Phi_{res\ n}=(0.060\pm0.002)\Phi_{thr\ n}$, the value of the resonance integral for the activation of $^{54}Fe$ by the $(n,\alpha)$ reaction was derived to be RI=(1.09±0.13) mb.

As a result of this combined experimental and theoretical investigation, it is concluded that it is impossible to produce appreciable amounts of $^{51}Cr$ by means of thermal neutron activation of $^{54}Fe$ under conditions existing in the first cooling loop of the IAE reactor.

## REFERENCES


[1] ALIYEV, A.I., et al., Nuclear Data for Neutron Activation Analysis - Reference Data, Atomizdat, Moscow (1969) (in Russian).

[2] MITEREV, A.I., et al., At.Ehnerg. 31 3 (1971) 281. (in Russian).

[3] GERASSIMOV, V.V., et al., Water Cooled Nuclear Power Plants, Atomizdat, Moscow (1976) (in Russian).

[4] ROCHLIN, C.H., Nucleonics 17 (1959) 55.

[5] INTERNATIONAL ATOMIC ENERGY AGENCY, Mtg. Proc. on Chemistry Research and Chemical Techniques Based on Chemistry Research Using Research Reactors, IAEA, Vienna (1963).

[6] MELLISH, C.E., et al., Radioisotopes in Scientific Research (Proc. Int. Conf. Paris, 1957), Pergamon Press.

[7] Nuclear Physics Reference Data (Transl. from English, ARTSIMOVICH, L.A., Transl.) Gosizdat, Moscow (1963) (in Russian).

[8] BYCHKOV, V.M., et al., Neutron Induced Threshold Reaction Cross-Sections - Reference Data, Ehnergoizdat, Moscow (1982) (in Russian).

[9] KHAID, Eh., et al., "Nuclear Properties of Heavy Elements", Atomizdat, 3 (1968) 134,157 (in Russian).

[10] PIK-PITCHAK, G.A., et al., Yad. Fiz. 44 (1986) 1421 (in Russian).

[11] BOR, O., MOTTELSON, B., The Structure of the Atomic Nucleus, Mir, Moscow, 1 (1971) 154 (in Russian).

[12] JOHANSON, P.I., et al., (Proc. Int. Conf. on Nuclear Cross-Sections and Technology, Washington, DC, 1975), NBS Special Publication 425 (1975) 572.

[13] GUSSEV, N.G., DMITRIEV, P.P., Quantum Radiation from Radioactive Nuclides - Reference Data, Atomizdat, Moscow, (1977) (in Russian).

[14] RODIONOV, Yu.F., YASHIN, Yu.A., Problems of Atomic Science and Technology. Ser. Nuclear Constants, 2 (1989) 50 (in Russian).

[15] MUGHABHAB, S.F., et al., Neutron Cross-Sections, Vol.1, Academic Press, New York (1981).

# ISOTOPIC DEPENDENCE OF RADIATIVE CAPTURE CROSS-SECTIONS FOR 30 keV NEUTRONS

Yu. N. Trofimov
V.G. Khlopin Radium Institute, Leningrad

Abstract

The average neutron radiative capture cross-section for 32 stable and 51 radioactive nuclides have been evaluated at 30 keV.

Neutron radiative capture cross-sections (P3) data at 30 keV are primarily of interest to astrophysicists investigating the application of the S-process to nucleo-synthesis. Information on these cross-sections is needed for stable and radioactive nuclides having masses larger than A=50. At the present time, there exists a vast amount of information on these cross-sections for medium and heavy mass nuclides [1-12]. Various versions of these data are contradictory because they are based on different initial evaluation principles, for instance:

- that the production of P3 cross-sections and the isotopic comtent of neighboring masses must be more or less constants [2];
- that calculations using the Hauser-Feshbach statistical model, can predict unknown cross-section to an accuracy of not better than 100% [3];
- that an estimation of unknown cross-sections can be obtain from the knowledge of the cross-section of the heaviest isotope of the same element [4];
- that the cross-section is semi-empirically dependent on the number of neutrons in the target nucleus [5,6];
- that evaluated data can be used in evaluations [7,8].

As a result of an analysis of our own P3 cross-section data, in the energy range of 0.5 to 2 MeV, of 54 stable isotopes of different elements [9], as well as other data taken from the literature [1], it was shown that the magnitude of the P3 cross-section decreases as the neutron excess of nuclei increases. The

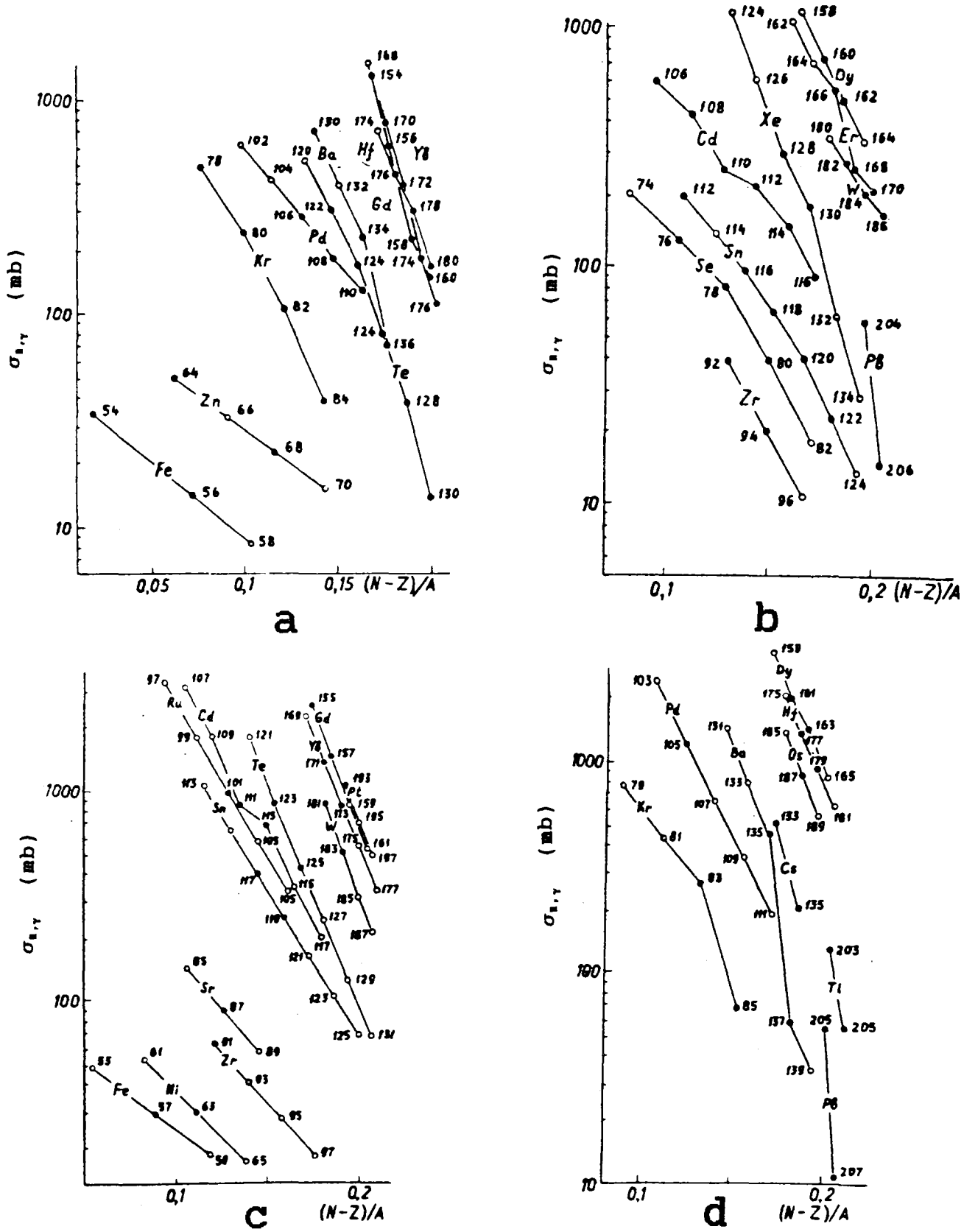


Dependence of the neutron-induced P3 cross-section for 30 keV neutrons on the neutron excess parameter.

a) and b) - even-even nuclei;
c) and d) - even-odd nuclei;
• - experimental data;
o - results of this evaluation.

following dependence was formulated on the basis of this P3 cross-section analysis:

$$\sigma_{\alpha} = \sigma_{o} \exp(-K\alpha)$$

where $\sigma_{\alpha}$ and $\sigma_{0}$ are the P3 cross-sections for isotopes having a neutron excess parameter $\alpha$=(N-Z)/A and $\alpha$=0(N=Z) respectively, K is a constant, and N and Z are the neutron and proton numbers of the nucleus.

In order to check the validity of this relationship at a neutron energy of 30 keV, the logarithm of the P3 cross-sections was plotted against the (N-Z)/A parameter for three different groups of target nuclei (e.g., even-even, even-odd, and odd-even). Data published in reference [1] were used as reference data. The plots of these graphs are shown in Figures a,b,c, and d below; it can be seen that most experimental data agree with the isotopic dependence proposed above. Although the same relationship was applied to magic number target nuclei (N=50,82,126), and for those nuclei which undergo a shape change, the data used in the comparison were based on the isotone analogs of different elements (i.e., nuclei having the same number of neutrons).

This isotopic relationship can be used not only to discard conflicting or questionable data, but can also be used to predict cross-section values for nuclei for which there are no data, including radioactive target nuclei. The reference data to be used for the evaluation of the P3 cross-sections at a neutron energy of 30 keV for each element was selected in the following manner:

- the analysis of the data was done separately for each parity group;
- in the case of conflicting cross-section information, all of the data for the whole chain of isotopes for a given element (selecting only those experimental results which obey the isotopic dependency rule) were used in the analysis. These cross-section were then used as reference data in the evaluation of unknown P3 cross-sections of other isotopes.

The results of the evaluation based on the isotopic dependence relationship (identified in the Figures by the open circles) of the P3 cross-sections at 30 keV, for those nuclei whose data differ significantly with existing data or for those whose data are lacking altogether, are listed in Tables 1 and 2. The evaluation of the P3 cross-sections at 30 keV was performed first for the following isotopes: $^{55,59}Fe$, $^{65}Ni$, $^{70}Zn$, $^{76}Ge$, $^{79}Kr$, $^{85,89}Sr$, $^{95,97}Zr$, $^{97,105}Ru$, $^{125}Sn$, $^{121,129}Te$, $^{126,127,131,133}Xe$, $^{139}Ba$, $^{159}Dy$, $^{161}Gd$, $^{163,164}Er$, $^{177}Yb$ and $^{195,197}Pt$.

TABLE 1. AVERAGED P3 CROSS-SECTIONS FOR 30 KEV NEUTRONS OF MEDIUM AND HEAVY MASS STABLE NUCLEI EVALUATED ON THE BASIS OF THE ISOTOPIC DEPENDENCE. (data given in mb = $10^{-31}$m)

| Isotope | $\sigma_{n,\gamma}(\Delta\sigma_{n,\gamma})$ | | Reference reaction data | |
|---|---|---|---|---|
| | Present evaluation | Results of other authors | Isotope | $\sigma_{n,\gamma}(\Delta\sigma_{n,\gamma})$ |
| $^{51}Fe$ | 8.1(1.2) | 8.5 [7]<br>14.3(1.4) [1] | $^{54}Fe$<br>$^{56}Fe$ | 34(3)<br>13.9(1.1) |
| $^{72}Ge$ | 35(5) | 33.9 [7] | $^{70}Ge$ | 75(22) |
| $^{74}Ge$ | 17(3) | 25 [2] | - | - |
| $^{76}Ge$ | 7(1) | none | - | - |
| $^{74}Se$ | 200(40) | 380(190) [10] | $^{76}Se$ | 129(60) |
| $^{82}Se$ | 18(4) | 12(3) [10] | $^{78}Se$ | 80 |
| - | - | 14(5) [10] | $^{80}Se$ | 40 |
| $^{84}Sr$ | 148(20) | 160(30) [10] | $^{86}Sr$ | 70(8) |
| $^{96}Zr$ | 11(2) | 41 [1] | $^{92}Zr$ | 43(10) |
| - | - | - | $^{92}Zr$ | 27(3) |
| $^{99}Ru$ | 1826(200) | 1100 [2] | $^{101}Ru$ | 1011(40) |
| $^{102}Pd$ | 614(100) | 770(110) [10] | $^{106}Pd$ | 284(30) |
| $^{104}Pd$ | 420(50) | 447(23) [11] | $^{108}Pd$ | 180(20) |
| - | - | 300(20) [1] | $^{110}Pd$ | 127(10) |
| $^{114}Sn$ | 137(20) | 135(20) [5] | $^{112}Sn$ | 202(24) |
| $^{124}Sn$ | 13.4(3.0) | 23.4 [1] | $^{116}Sn$ | 97(19) |

TABLE 1. AVERAGED P3 CROSS-SECTIONS FOR 30 KEV NEUTRONS OF MEDIUM AND HEAVY MASS STABLE NUCLEI EVALUATED ON THE BASIS OF THE ISOTOPIC DEPENDENCE. (data given in mb = $10^{-31}$m)

| | | | | |
|---|---|---|---|---|
| - | - | - | $^{118}$Sn | 65(12) |
| - | - | - | $^{120}$Sn | 41(7) |
| - | - | - | $^{122}$Sn | 23(5) |
| $^{115}$Sn | 665(80) | 560(90) [10] | $^{117}$Sn | 418(70) |
| - | - | - | $^{119}$Sn | 257(60) |
| $^{120}$Te | 518(100) | 210(20) [10] | $^{122}$Te | 305(60) |
| - | - | - | $^{124}$Te | 169(20) |
| - | - | - | $^{126}$Te | 80 |
| - | - | - | $^{128}$Te | 38 |
| - | - | - | $^{130}$Te | 14 |
| $^{124}$Xe | 1150(300) | 1153(110) [8] | $^{128}$Xe | 300(150) |
| $^{126}$Xe | 600(200) | none | $^{130}$Xe | 180(50) |
| $^{132}$Xe | 60(20) | 61(4) [8] | - | - |
| $^{134}$Xe | 29(10) | 29(2) [8] | - | - |
| $^{131}$Xe | 320(100) | none | $^{129}$Xe | 666 [7] |
| $^{132}$Ba | 395(60) | 540(40) [10] | $^{130}$Ba | 715(58) |
| - | - | - | $^{134}$Ba | 252(35) |
| - | - | - | $^{136}$Ba | 70(10) |
| $^{158}$Dy | 1164(200) | 1350(170) [10] | $^{160}$Dy | 740(40) |
| $^{164}$Dy | 330(60) | 300(50) [5] | $^{162}$Dy | 490(50) |
| $^{162}$Er | 1053(150) | 1135(80) [10] | $^{170}$Er | 208(25) |
| $^{164}$Er | 645(90) | none | - | - |
| $^{166}$Er | 437(80) | 558(54) [1] | - | - |
| $^{168}$Er | 300(5) | 243(73) [7] | - | - |
| $^{168}$Yb | 1450(200) | 1490(130) [5] | $^{170}$Yb | 738(29) |
| $^{178}$Yb | 55(10) | 57(7) [5] | $^{172}$Yb | 402(33) |
| - | - | - | $^{174}$Yb | 183(16) |
| - | - | - | $^{176}$Yb | 110(11) |
| $^{180}$W | 344(40) | 350(20) [5] | $^{182}$W | 273(14) |
| - | - | - | $^{184}$W | 206(10) |
| - | - | - | $^{186}$W | 170(9) |
| $^{189}$Os | 555(100) | 858 [7] | $^{187}$Os | 874(28) |
| $^{195}$Pt | 728(100) | none | $^{193}$Pt | 1100 [12] |

TABLE 2. AVERAGED P3 CROSS-SECTIONS FOR 30 KEV NEUTRONS OF MEDIUM AND HEAVY MASS RADIOACTIVE NUCLEI EVALUATED WITH THE USE OF THE ISOTOPIC DEPENDENCE. (data given in mb = $10^{-31}$m)

| Isotope | $\sigma_{n,\gamma}(\Delta\sigma_{n,\gamma})$ | | Reference reaction data | |
|---|---|---|---|---|
| | Present evaluation | Results of other authors | Isotope | $\sigma_{n,\gamma}(\Delta\sigma_{n,\gamma})$ |
| $^{55}$Fe | 48(10) | none | $^{57}$Fe | 29.5 [7] |
| $^{59}$Fe | 19(5) | none | - | - |
| $^{79}$Kr | 862(170) | none | $^{83}$Kr | 272 |
| $^{81}$Kr | 602(120) | 450 [12] | - | - |
| $^{85}$Sr | 145(30) | none | $^{87}$Sr | 91(15) |
| $^{89}$Sr | 58(12) | none | - | - |
| $^{93}$Zr | 41(12) | 70 [12] | $^{91}$Zr | 64(8) |
| $^{95}$Zr | 28(10) | none | - | - |
| $^{97}$Zr | 18(5) | none | - | - |
| $^{97}$Ru | 3300(1000) | none | $^{101}$Ru | 1011(40) |
| $^{103}$Ru | 590(120) | 744 [7] | - | - |
| $^{105}$Ru | 340(70) | none | - | - |
| $^{103}$Pd | 2440(800) | 1590(190) [5] | $^{105}$Pd | 1246(130) |
| $^{107}$Pd | 658(100) | 680(50) [5] | - | - |
| $^{109}$Pd | 483(80) | 465(25) [5] | - | - |
| $^{111}$Pd | 190(60) | 307(14) [5] | - | - |
| $^{107}$Cd | 3165(1000) | 1830(230) [5] | $^{111}$Cd | 880(125) |
| $^{109}$Cd | 1882(360) | 1200(120) [5] | $^{113}$Cd | 715(80) |
| $^{115}$Cd | 358(50) | 400(50) [5] | - | - |
| $^{117}$Cd | 204(30) | 300(15) [5] | - | - |
| $^{113}$Sn | 1096(200) | 1130(210) [10] | $^{117}$Sn | 418(70) |
| $^{121}$Sn | 167(25) | 161(12) [5] | $^{119}$Sn | 257(60) |
| $^{123}$Sn | 107(15) | 112(7) [5] | - | - |
| $^{125}$Sn | 70(10) | none | - | - |
| $^{121}$Te | 1853(220) | none | $^{123}$Te | 913(91) |
| $^{127}$Te | 247(50) | 200 [10] | $^{125}$Te | 450 |
| $^{129}$Te | 129(25) | none | - | - |
| $^{131}$Te | 69(15) | 193(16) [10] | - | - |
| $^{127}$Xe | 1340(250) | none | $^{129}$Xe | 666 [7] |
| $^{133}$Xe | 156(30) | none | - | - |

TABLE 2. AVERAGED P3 CROSS-SECTIONS FOR 30 KEV NEUTRONS OF MEDIUM AND HEAVY MASS RADIOACTIVE NUCLEI EVALUATED WITH THE USE OF THE ISOTOPIC DEPENDENCE. (data given in mb = $10^{-31}$m)

| | | | | |
|---|---|---|---|---|
| $^{131}$Ba | 1465(300) | 1400 [10] | $^{135}$Ba | 465(80) |
| $^{135}$Ba | 812(200) | 800 [10] | $^{137}$Ba | 58(10) |
| $^{153}$Gd | 4400(1000) | 2500 [12] | $^{155}$Gd | 2620(260) |
| $^{159}$Gd | 900(150) | 875(100) [10] | $^{157}$Gd | 1510(140) |
| $^{161}$Gd | 544(80) | none | - | - |
| $^{159}$Dy | 3327(600) | none | $^{161}$Dy | 2010(90) |
| $^{165}$Dy | 845(200) | 500(50) [10] | $^{163}$Dy | 1450(150) |
| $^{163}$Er | 3900(1000) | none | $^{167}$Er | 1439 [7] |
| $^{165}$Er | 2440(500) | 2845(360) [5] | - | - |
| $^{169}$Er | 900(150) | 660(30) [5] | - | - |
| $^{171}$Er | 141(17) | 124(15) [5] | $^{170}$Er | 208(25) |
| $^{169}$Yb | 2320(300) | 2580(110) [5] | $^{171}$Yb | 1411(51) |
| $^{175}$Yb | 566(90) | 390(40) [5] | $^{173}$Yb | 885(75) |
| $^{177}$Yb | 344(50) | none | - | - |
| $^{175}$Hf | 2060(500) | 2000(650) [5] | $^{177}$Hf | 1366(61) |
| $^{181}$Hf | 614(100) | 450(70) [5] | $^{179}$Hf | 940(80) |
| $^{181}$W | 900(200) | 620(35) [5] | $^{183}$W | 531(26) |
| $^{185}$W | 320(50) | 342(10) [5] | - | - |
| $^{187}$W | 213(30) | 257(7) [5] | - | - |
| $^{185}$Os | 1394(200) | 1220(100) [5] | $^{187}$Os | 874(28) |
| $^{197}$Pt | 503(150) | none | $^{193}$Pt | 1100 [12] |

## REFERENCES


[1] BELANOVA, T.S., IGNATYUK, A.V., PASHCHENKO, A.B., PLYASKIN, V.I., Fast Neutron Radiative Capture, Ehnergoatomizdat, Moscow (1986) (in Russian).

[2] CONRAD, J., Thesis, Heidelberg (1976).

[3] HOLMES, J.A., WOOSLEY, S.F., FOWLER, W.A., ZIMMERMAN, B.A., At. Data Nucl. Data Tables 18 (1976) 305.

[4] LYUTOSTANSKIJ, Yu.S., PTITSYN, D.A., SINYUKOVA, O.N., FILIPPOV, S.S., CHECHETKIN, V.M., Preprint No.95, M.V. Keldysh IPM Institute (1984) (in Russian).

[5] NEDVEDYUK, K., LASSON, L., POPOV, Yu., Neutron Physics, TsNIIAtominform (1988) (in Russian).

[6] BELANOVA, T.S.,GORBACHEVA, L.V., GRUDZEVICH, O.T., IGNATYUK, A.V., MANTUROV, G.N., PLYASKIN, V.M., At.Ehnerg. 57 (1984) 243 (in Russian).

[7] NEWMAN, M.J., Astrophys.J. 219 (1978) 676.

[8] CHECHEV, V.P., KRAMAROVSKY, Ya.M., Usp. Fiz. Nauk 134 (1981) 431 (in Russian).

[9] TROFIMOV, Yu.N., Problems in Atomic Science and Technology. Ser. Nuclear Constants 4 (1987) 10 and 2 (1989) 11 (in Russian).

[10] NEDVEDYUK, K., POPOV, Yu., Neutron Physics, TsNIIAtominform, Moscow (1984) (in Russian).

[11] KAEPPELER, F., BEER, H., WISSHAK, K., CLAYTON, D.D., MACKLIN, R.I., WARD,R.A., Astrophys.J. 257 (1982) 821.

[12] KRAMAROVSKIJ, Ya.M., CHECHEV, V.P., Element Synthesis in the Universe, Nauka, Moscow (1987).

# EVALUATION OF PARTICLE EMISSION SPECTRA FOR ISOTOPES OF CHROMIUM, IRON AND NICKEL FOR THE BROND DATA LIBRARY

A.V. Zelenetskij
Nuclear Energy Institute, Obninsk

A.B. Pashchenko
Institute of Physics and Power Engineering, Obninsk

## Abstract

New evaluation results for spectra of neutron proton, and alpha-particle emission for Cr, Fe and Ni isotopes are presented. New approaches for the description of the non-statistical part of the reaction mechanism and inverse cross-sections are discussed. The results of this evaluation have been incorporated in the BROND evaluated data library.

## Introduction

The theoretical analysis of nuclear reaction cross-sections and particle emission spectra are widely used in neutron nuclear data evaluation. Of prime importance in this regard is the appropriateness of the theoretical models for the various types of nuclear reactions and the energy range of the incident neutrons, as well as the influence of the model parameters on the accuracy of the calculations.

At the root of the theoretical approach to the description of nuclear reactions in the medium energy range, is the separation of the mechanisms of the interaction of the incident particle with the target nucleus into direct, pre-equilibrium and equilibrium processes. The contribution of each of these processes varies according to the properties of the individual nuclei, the interaction energy, the type of reaction, and can also depend to some extent on the experimentally determined energy and angular distributions of the reaction products. Until now, methods have been developed which allow the evaluation of

the contributions of the various processes to give a reliable description of the (n,n') and (n,p) reactions mechanisms. Currently, the least substantiated is the non-equilibrium stage of nuclear reactions which have complex particles in their output channels, i.e., particles made up of a few nucleons. One of the most important of such reactions is the (n,$\alpha$) reaction which leads to the production and accumulation of helium, which plays a significant role in a number of applied problems (such as damage to nuclear reactor materials, internal reactor dosimetry, etc.). The importance to take the non-equilibrium component of nuclear reactions into account is not questioned any more [1]. The non-statistical component of nuclear reactions are nowadays considered as the sum of direct (DMT) and compound (CMT) multistep transitions [2]. Exact DMT calculations are very complicated and require large amounts of computer time, even for the case of simple nucleons in the output channel. For this reason, the evaluation of the non-statistical component of nuclear reactions is performed exclusively in the framework of CMT calculations, and in order to calculate the contribution of the non-equilibrium reaction mechanism, a variety of modified exciton models of pre-equilibrium particle emission have been developed. Research in this direction has led to the appearance of developed pre-equilibrium reaction models whose results are in good agreement with experimental data [3-6].

Nevertheless, as shown in reference [7], it is impossible to calculate the non-equilibrium component exclusively in the framework of CMT calculations and arrive at a satisfactory description for both cross-sections and particle emission spectra for the (n,p), (n,$\alpha$) and (n,2n) reactions with a single value of the K parameter - the average root-mean-square of the matrix element - which is normally described by the following equation [8]:

$$\langle |M|^2 \rangle = K A^{-3} E^{-1}$$

It was shown in reference [9] that good agreement between theoretical and experimental values simultaneously for the proton and neutron output channels could be obtained with a single value of the K parameter equal to 700 $MeV^3$, by taking into account

direct coherent transitions which excite the collective states of the residual nucleus in addition to the pre-equilibrium component for the neutron channel. However, the question concerning the connection between the pre-equilibrium and direct components in the (n,$\alpha$) reaction remains unresolved.

In this work we have performed the analysis of particle emission spectra, simultaneously in neutron, proton, and alpha reaction channels, using the same approach described in reference [9]. The first part of this article analyzes the applicability of the pre-equilibrium complex particle emission model, developed by the authors of reference [6], to the description of alpha cluster emission spectra in neutron-induced nuclear reactions. The connection between the pre-equilibrium and direct reaction mechanisms is considered in the second part of this article, and the results obtained with a new approach to describe inverse reactions in charged particle channels are presented in the third part of the article.

## Pre-equilibrium particle emission

The contribution of the pre-equilibrium mechanism in particle emission was calculated initially using the model proposed in reference [9], which in contrast to earlier proposed models, described in references [3-5], gives the possibility to analyze emission spectra of simple particles (neutrons and protons) as well as complex particles (d, t, $\alpha$, and others) by using a single approach. For simple particles, the prediction of this model is the same as that of the traditional models. In the emission of complex particles consideration must be given not only to the contribution of the particle yield mechanism, but also to the inputs, such as the pickup of the target nucleus by the incoming particle. The basic aspects of this approach are described in the following.

It is assumed that the complex particle (cluster) can be formed not only from quasi-particles excited above the Fermi level, but also from quasi-particles populating various states of the compound system which lie below the Fermi level. The probability of cluster formation from *l* excited and *m* non-excited quasi-

particles ($l + m = p$ - the number of nucleons in the cluster) is defined as the integral of the wave function of the cluster $\varphi_c$ superimposed by the $p$ wave functions of each of the component nucleons $\varphi_i$ [6]. As an example, for an alpha cluster we have:

$$F_{l,m}(E_\alpha) = \sum_{\substack{s_j > s_F (i=1,l) \\ s_j < s (j=1,m)}} |\langle \varphi_c \chi^{(s)}(R) | \varphi_1 \varphi_2 \varphi_3 \varphi_4 \rangle|^2 \qquad (1)$$

In the evaluation of this expression reported in reference [6], the additional assumption is made that the cluster is formed somewhere in the surface layer of the nucleus; as a result, the summation over all modes of clusterization $(l,m)$ of the probability $F_{l,m}(E_\alpha)$ is smaller than one because of the limitation imposed on the phase space of the system.

This additional assumption can be expressed by the following equation:

$$|r_i| \leq R_0 \qquad (2)$$

where $r_i$ is the coordinate of the ith nucleon, and the value of $R_0$ - the radius of the compound nucleus - is defined by the following expression:

$$R_0 = R_{res} + \Delta R \qquad (3)$$

where $R_{res}$ - is the radius of the residual nucleus, and $\Delta R$ is the parameter which characterizes the thickness of the surface layer of the nucleus implying that the nucleus has a diffuse surface.

The results of the evaluation of the expression for $F_{l,m}(E_\alpha)$, which was performed in the work reported in reference [6] in the framework of the Fermi gas model formalism, are shown in Fig. 1. As indicated in reference [6], in context of the assumptions which were made in the evaluation of equation (1), the functional dependence of $F_{l,m}(E_\alpha)$ on $E_\alpha$ is invariant with respect to the quantity $\Delta R$, and the only effect that $\Delta R$ has is a change of the common normalizing factor. In this context, for $\Delta R \gg r_i$, where $r_i$=1.6 fm is the experimental root mean square value of the alpha-particle radius, we have:

$$\sum_{l+m=4} F_{l,m}(E_\alpha) = 1 \qquad (4)$$

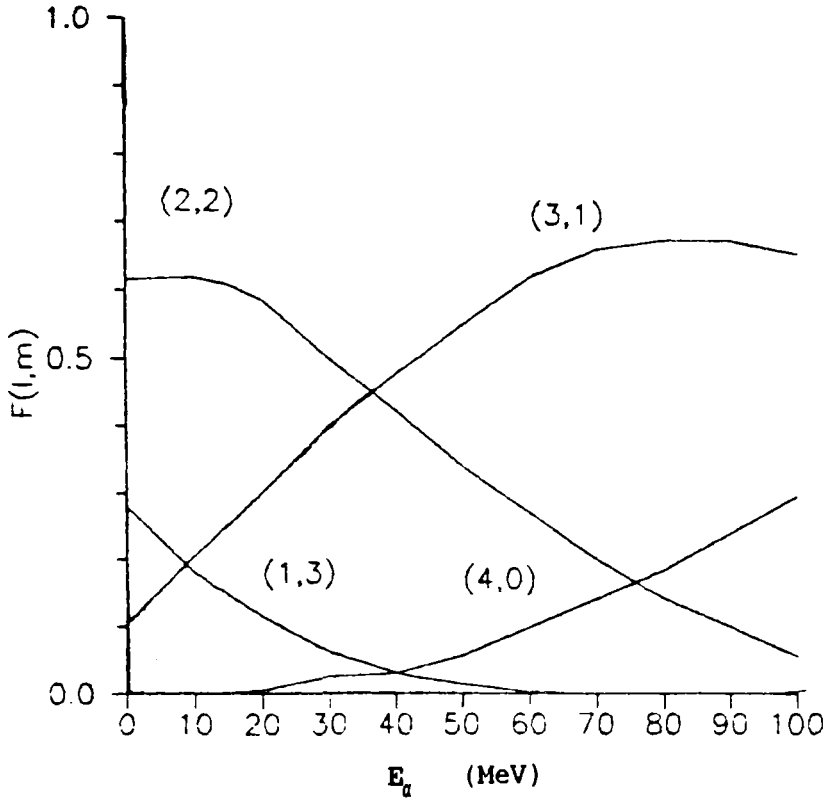


Fig. 1 Alpha-particle clusterization form factor [6].

so that for $\Delta R$=1.6 fm and for $\Delta R$=1 fm the sum given by (4) is equal to 0.94 and 0.41 respectively, and approaches 0 as $\Delta R \to 0$ fm.

The rate at which the n-exciton state decays by the alpha-cluster (l,m) emission mode can be expressed by the following equation:

$$W(n,l,m,E_\alpha) = \left[\frac{(2S_\alpha+1)}{\pi^2\hbar^3}\right] \mu_\alpha E_\alpha \sigma_{inv}(E_\alpha)\, \varphi(\Delta R)\, \Psi \qquad (5)$$

where

$$\Psi = \frac{F_{l,m}(E_\alpha)\, \omega(p-1,h,U)}{\omega(p,h,E)}$$

and where all of the terminology is the same as in reference [6].

Equation (5) differs from the corresponding equation (2.19) of reference [6] in that the dependence of $F_{l,m}(E_\epsilon)$ on the $\Delta R$ parameter is presented here explicitly by the $\varphi(\Delta R)$ factor, and the values of $F_{l,m}(E_\epsilon)$ in equation (5) correspond to the extreme case of $\Delta R \gg r_\epsilon$ (see Fig.1).

Analysis of experimental alpha-particle emission spectrum data obtained from the (n,$\alpha$) reaction measured between 29 MeV and 62

MeV for the $^{54}Fe$ and $^{118,124}Sn$ nuclides by the authors of reference [6], shows good agreement between the experimental values and the spectra calculated with the parameter $\Delta R=1$ fm, which corresponds to the value $\varphi(\Delta R)=0.4$ in equation (5).

However, the following should be noted with respect to the method used in this analysis. First one must note that in calculating the form-factors $F_{l,s}(E_c)$ in reference [6] the authors used nucleons which did not bear any relation to the composite cluster particles. As a result, the $F_{l,s}(E_c)$ coefficients are based only on the quantitative composition of the cluster and on the energy state of the composite nucleons with respect to the Fermi level.

The modified form of equation (5), which gives the possibility to differentiate between neutrons and protons in the formation of emitting clusters from compound systems, was derived in the work described in reference [10]. In that derivation, the expressions for the density of quasi-static states $\omega(p-1,h,U)$ and $\omega(p.h,E)$, obtained in a single fermion approximation with a density of single particle states g, was replaced in equation (5) by having densities corresponding to single-particle states $g_\nu$ and $g_\pi$ for the neutron and proton components, respectively. The factor can be represented in a simple convenient form if one assumes that $g_\nu=K_\nu g$ and $g_\pi=K_\pi g$, where $K_\nu$ and $K_\pi$ are constants (which are normally taken to be equal to $K_\nu=K_\pi=\frac{1}{2}$). The density of quasi-static states of a two-component Fermi gas can thus be represented by the expression [11]:

$$\omega(\nu,\pi,E)=\frac{g(gE)^{n-1}}{K_\nu^{\nu+\bar{\nu}}\,K_\pi^{\pi+\bar{\pi}}\,\nu!\bar{\nu}!\pi!\bar{\pi}!} \tag{6}$$

where $\nu$, $\bar{\nu}$, $\pi$ and $\bar{\pi}$ are the number of neutron- and proton-type particles and holes, respectively, and

$$p=\nu+\pi\ ,\quad h=\bar{\nu}+\bar{\pi}\ ,\quad n=p+h \tag{7}$$

Expression (6) can be rewritten as:

$$\omega(\nu,\pi,E)=K(\nu,\pi)\,\omega(p,h,E) \tag{8}$$

where

$$K(\nu,\pi)=p!h!\,/\,K_\nu^{\nu+\bar{\nu}}\,K_\pi^{\pi+\bar{\pi}}\,\nu!\bar{\nu}!\pi!\bar{\pi}! \tag{9}$$

Summing over all of the resolved configurations in the residual and compound systems, and complying with the conditions given in (7), we obtain:

$$\omega'(p-1,h,U) = \omega(p-1,h,U) \sum_{N_R} K(\nu,\pi,l,m) \qquad (10)$$

and

$$\omega'(p,h,E) = \omega(p,h,E) \sum_{N_C} K(\nu,\pi) \qquad (11)$$

where the $N_R$ and $N_C$ indexes take all of the resolved configurations in the residual and compound systems into account.

Substituting equations (10) and (11) in (5), we obtain:

$$W(n,l,m,E_\alpha) = \left[\frac{2S_\alpha+1}{\pi^2\hbar^3}\right] \mu_\alpha E_\alpha \sigma_{inv}(E_\alpha)\, \varphi(\Delta R)\, F_{l,m,}(E_\alpha)\, \Psi \qquad (12)$$

where

$$\Psi = \frac{K_R(p,h,l,m)\, \omega(p-1,h,U)}{K_C(p,h)\, \omega(p,h,E)}$$

and

$$K_R(p,h,l,m) = \sum_{N_R} K(\nu,\pi,l,m) \qquad (13)$$

and

$$K_C(p,h) = \sum_{N_C} K(\nu,\pi) \qquad (14)$$

The $K_R(p,h,l,m)$ and $K_C(p,h)$ can be easily evaluated for any given (l,m) clustering mode in a (p,h) state. The numerical values of these coefficients, calculated up to n=21 and assuming that $K_\nu = K_\pi = \frac{1}{2}$, are listed in the Table below.

A comparison of experimental and calculated alpha-particle emission spectra calculated with equation (12) are shown in Figs 2 and 3. It can be seen from these figures that the agreement between the experimental and calculated data is achieved for the value of $\varphi(\Delta R) \approx 0.1$.

TABLE OF NUMERICAL VALUES OF THE $K_C$, $K_\nu$, $K_\pi$ AND $K_\alpha$ COEFFICIENTS

| n | p | h | $K_C$ | $K_\nu$ | $K_\pi$ | $K_\alpha$ (1.3) | $K_\alpha$ (2.2) | $K_\alpha$ (3.1) | $K_\alpha$ (4.0) |
|---|---|---|---|---|---|---|---|---|---|
| 3 | 2 | 1 | 0.375 | 0.500 | 0.250 | 0.500 | 0.750 | 0.000 | 0.000 |
| 5 | 3 | 2 | 0.312 | 0.375 | 0.250 | 0.507 | 0.812 | 0.750 | 0.000 |
| 7 | 4 | 3 | 0.273 | 0.312 | 0.234 | 0.480 | 0.781 | 0.625 | 0.375 |
| 9 | 5 | 4 | 0.246 | 0.273 | 0.218 | 0.447 | 0.726 | 0.546 | 0.312 |
| 11 | 6 | 5 | 0.225 | 0.246 | 0.205 | 0.418 | 0.673 | 0.492 | 0.273 |
| 13 | 7 | 6 | 0.209 | 0.225 | 0.193 | 0.392 | 0.627 | 0.451 | 0.246 |
| 15 | 8 | 7 | 0.196 | 0.209 | 0.183 | 0.370 | 0.588 | 0.418 | 0.225 |
| 17 | 9 | 8 | 0.185 | 0.196 | 0.174 | 0.352 | 0.556 | 0.392 | 0.209 |
| 19 | 10 | 9 | 0.176 | 0.185 | 0.166 | 0.336 | 0.528 | 0.370 | 0.196 |
| 21 | 11 | 10 | 0.168 | 0.176 | 0.160 | 0.322 | 0.504 | 0.352 | 0.185 |

In addition, the following can be said:

1. By taking the neutron-proton difference in the pre-equilibrium component into consideration, one can recognize some structure in the pre-equilibrium alpha-particle spectrum which is similar in shape to the structure in the region of the maxima of experimental spectra ($E_\alpha$ ≈ 7-9 MeV) which speaks for a general agreement between experiment and calculation.

2. On the other hand, we have not been able to achieve agreement between experimental and calculated spectra in the framework of the investigated theoretical model, particularly for hard alpha-particles in the quantified energy region of the spectrum ($E_\alpha$ ≈ 12-15 MeV). An increase in the contribution of pre-equilibrium alpha-particles at the expense of an increase in the value of the $\varphi(\Delta R)$ parameter, together with an improved description of the spectrum in the middle energy range ($E_\alpha$ ≈ 10 MeV) leads to a simultaneous degradation of the agreement between experiment and theory in the region of the spectrum maximum and in the upper energy range ($E_\alpha$ ≈ 12-15 MeV).

## The direct mechanism in the (n,α) reaction

It can be seen from the data plotted in Figs. 2 and 3 that the calculated data does not give a good description of the hard part of the spectrum. As suggested in reference [10], this disparity could be eliminated if one assumed that there is a considerable contribution from the direct reaction mechanism in this range. The collective contribution of direct processes to the alpha-particle emission cross-section was evaluated here, in accordance with reference [10], according to the empirical formula:

$$\sigma_{pr}(E_\alpha) = [d\sigma/dE_\alpha]_{obs}\,(U-E_{\alpha 0}) \qquad (15)$$

where $\sigma_{pr}(E_\alpha)$ is the collective contribution of direct processes, $[d\sigma/dE_\alpha]_{obs}$ is the observed differential (n,α) reaction cross-section in the hard part of the alpha spectrum at an energy of $E_\alpha \approx 15$ Mev, $E_{\alpha 0}$ the effective energy boundary and U is the maximum excitation energy of the residual nucleus.

As indicated in reference [10], the value of $[d\sigma/dE_\alpha]_{obs}$ can be evaluated to be approximately equal to 0.5-1.5 mb/MeV, and the value of the $E_{\alpha 0}$ parameter can be taken to be 6-7 MeV. From the data shown in Figs.2 and 3, it can be seen that this approach gives an adequate description of the whole spectrum.

## The selection of optical model parameters for the calculation of inverse reaction cross-sections

It is well known that the parameters used in the calculation of nuclear reaction cross-sections with the statistical theory are the nuclear level density, the cross-section for the absorption of the incident particle by the target nucleus, and the inverse reaction cross-section [12]. The existing systematics of nuclear level density parameters is reliable enough to be able to predict the values of level densities [13], and the absorption and inverse reaction cross-sections are normally calculated with the optical potential model [14]. Optical model parameters are chosen on the basis of how well they describe the experimental data on the scattering of particles by nuclei in their ground state. It is evident that such a procedure is, generally speaking, not correct with respect to the determination of

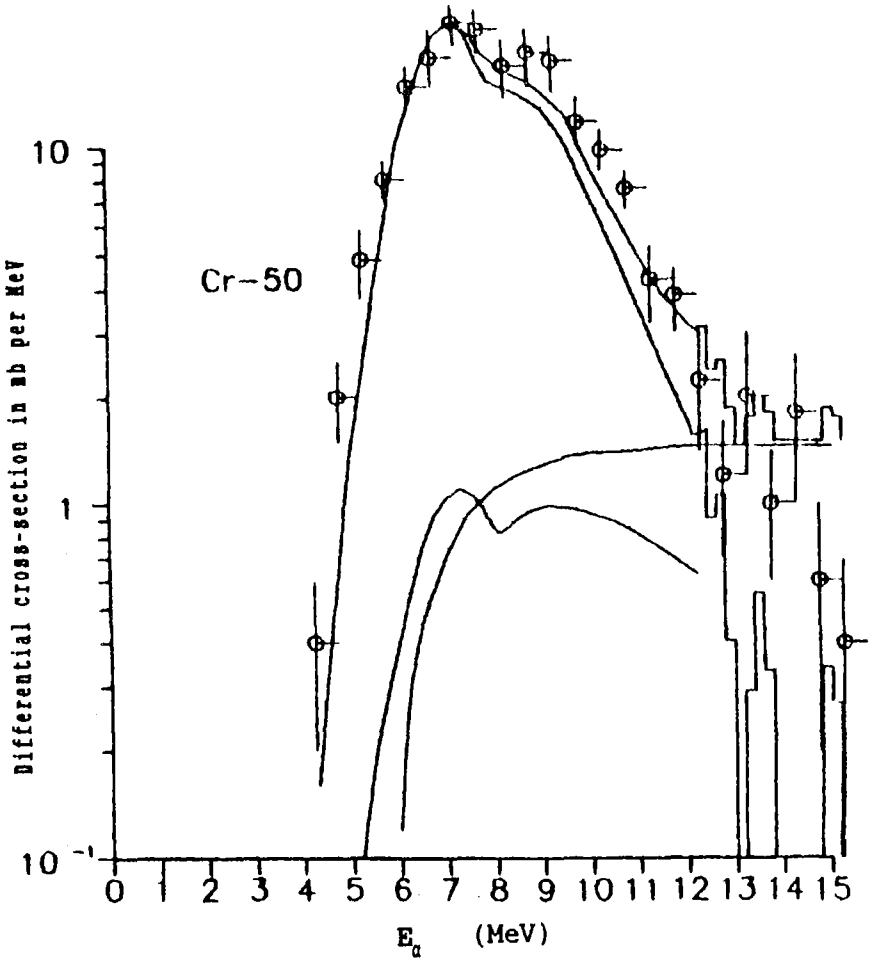


Fig. 2. Alpha-particle spectrum generated by the $^{50}Cr(n,\alpha)$ reaction at a neutron energy $E_n$ = 15 MeV.

Experimental data [18] - o

Calculated curves:
1 - pre-equilibrium spectrum;
2 - evaluated direct mechanism contribution;
3 - sum of equilibrium and pre-equilibrium;
4 - sum of equilibrium, pre-equilibrium and direct contributions.

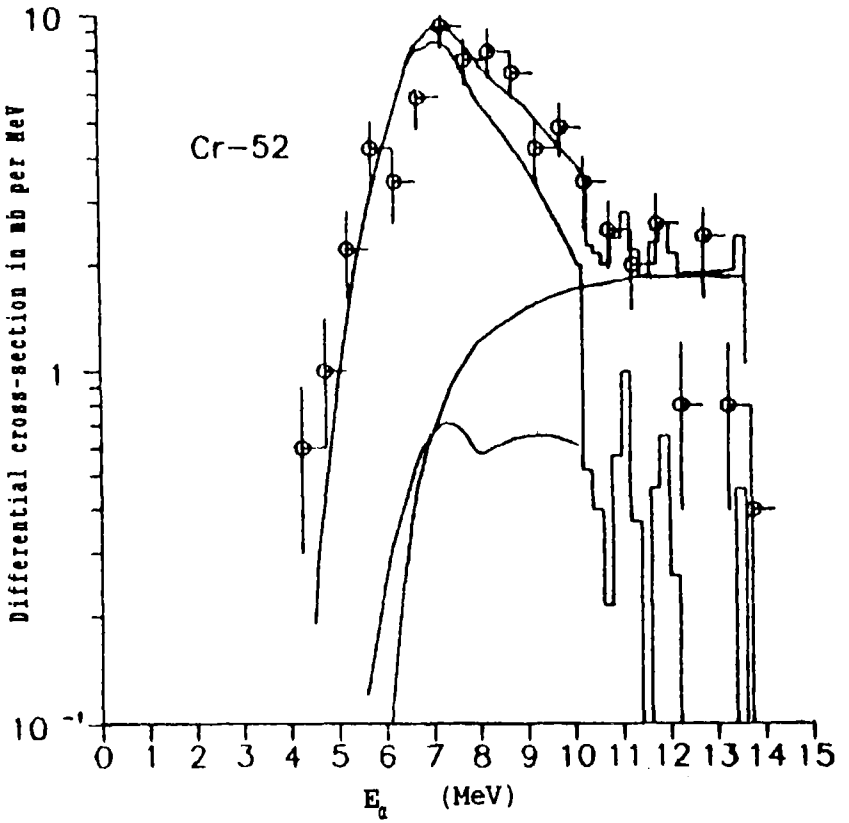


Fig. 3. Alpha-particle spectrum generated by the $^{52}Cr(n,\alpha)$ reaction at a neutron energy of $E_n$ = 15 MeV.

(Same caption designations as in Fig. 3.)

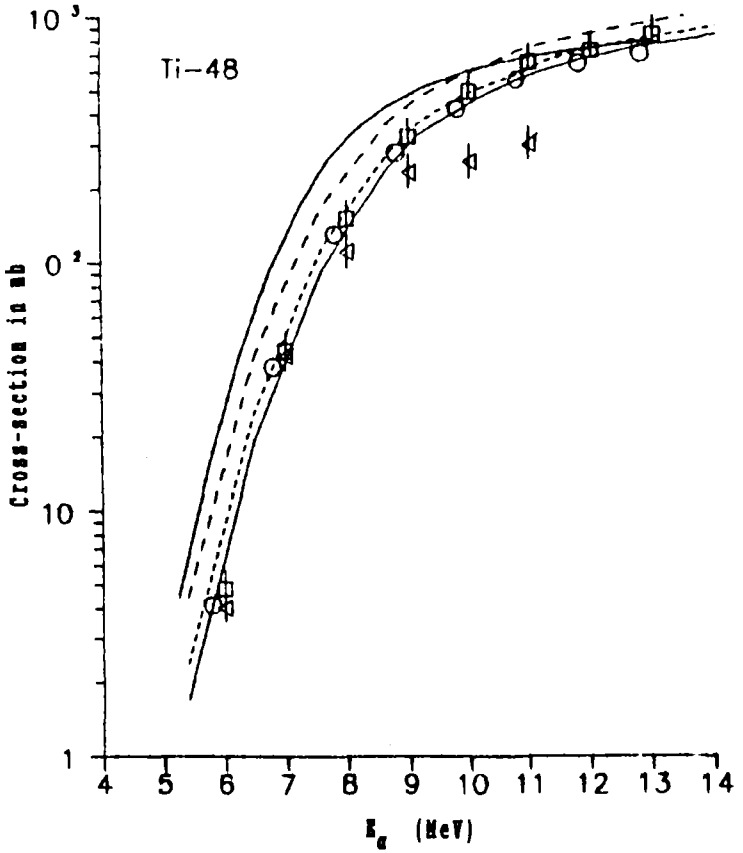


Fig. 4. Alpha-particle absorption cross-section.

Experimental data: ▲ - [19] , ○ - [20], □ - [20]

Calculated curves:
Lower continuous curve - reference [16] potential;
Upper continuous curve - reference [17] potential;
Dotted curve - reference [21] potential;
Dashed curve - reference [22] potential.

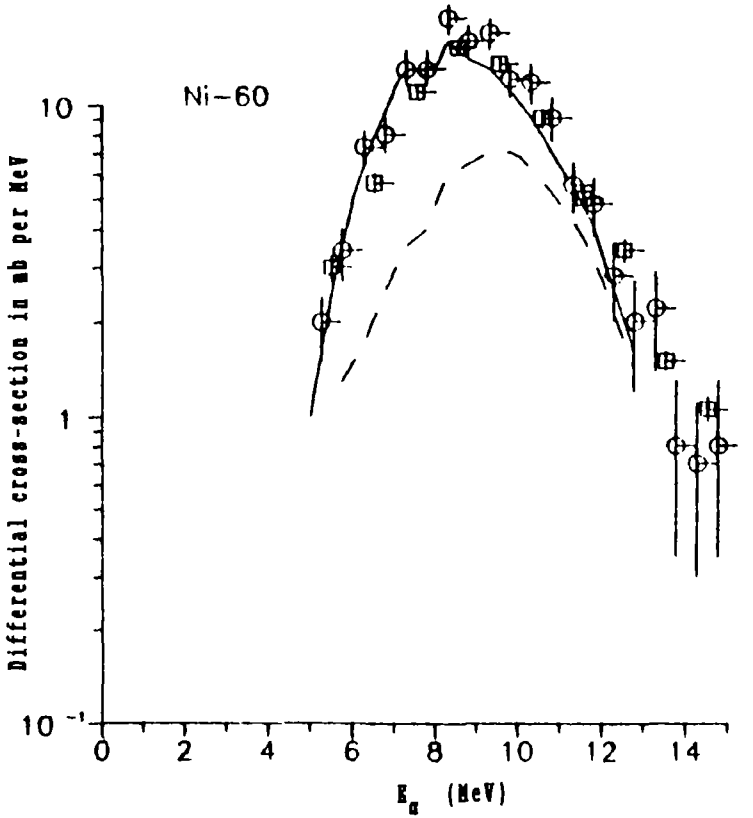


Fig. 5. Alpha-particle spectrum generated by the $^{60}Ni(n,\alpha)$ reaction at a neutron energy of $E_n$ = 15 MeV.

Experimental data: ○ - [18], □ -[23].

Calculated curves:
Continuous curve - reference [17] potential;
Dashed curve - reference [16] potential.

inverse reaction cross-sections, and to use absorption cross-sections calculated with the optical model in the capacity of inverse reaction cross-sections could lead to the wrong description of the cross-section and of the particle spectra. As an example, the work described in reference [15] reports a systematic difference between the theoretical and experimentally determined alpha-particle emission spectra in the low end of the spectrum. The investigation of this effect indicated that such a difference could not have been caused by an error in the determination of the energy level densities or by the wrong choice of the optical potential for the calculation of the transmission coefficients in the alpha channel of the reaction.

As an illustration, Fig. 4 shows the comparison of experimentally determined alpha-particle absorption cross-section data $\sigma_{abs}(E_\alpha)$ with cross-sections calculated with the optical model using standard potentials and an inverse reaction cross-section $\sigma_{inv}(E_\alpha)$ necessary to adequately describe alpha-particle emission spectra at 15 MeV incident neutron energies. This figure shows that at low alpha-particle energies, the value of $\sigma_{inv}(E_\alpha)$ differs significantly from the experimental alpha-particle absorption data, as well as from all calculated curves.

The authors of reference [15] interpreted these findings as a need to modify the alpha-particle transmission coefficients stipulated by the reduction of the height of the Coulomb barrier of the excited nucleus. The modification of the barrier was achieved in reference [15] by increasing the value of the diffusion parameter $a_R$ of the real part of the McFadden and Satchler [16] optical potential by 30-50 % for alpha-particle energies below the Coulomb barrier. The initial value of the $a_R$ parameter was used for energies above the Coulomb barrier, and the following expression was used to calculate the $a_R$ values in the intermediate energy range:

$$a_R(E_\alpha) = a_R^o + \frac{a_R^* - a_R^o}{1 + \exp\left[\frac{E_\alpha - E_{\alpha 0}}{\Delta E}\right]} \qquad (16)$$

where $a_R^*$ and $a_R^0$ are the increased and initial values of the $a_R$ parameter, respectively, $E_{\alpha 0}$ the parameter proportional to the

equivalent height of the Coulomb barrier, and $\Delta E$ the parameter defining the width of the intermediate energy range. The effect of reducing the effective barrier on the theoretical representation to describe experimental low energy end of alpha-particle spectra from (n,α) reactions at an incident neutron energy of 15 MeV is shown in Fig. 5. It must be noted that the value of the observed effect does not depend on the model of the level density used (as long as the parameters of these models yield data that are in agreement with the experimental data).

However, the energy dependence of $\sigma_{inv}(E_\alpha)$ which was derived in reference [15] has a significant limitation because it was determined for only one incident particle energy value, and consequently for only one single point of reference in the dependence of the excitation energy of the residual nucleus $U_r$ on the energy of the outgoing alpha-particle $E_\alpha$ represented by:

$$U_r = E_n \frac{\mu}{m} + Q_{n,\alpha} - E_\alpha \qquad (17)$$

where $\mu$ is the reduced mass, m the mass of the neutron, and $Q_{n,\alpha}$ the reaction energy.

As shown in reference [17], as $E_n$ increases, the difference between the inverse reaction cross-section and the alpha-particle absorption cross-section increases. In the evaluation of excitation functions or particle emission spectra at various incident particle energies, it is therefore absolutely necessary to know the behavior of the inverse reaction cross-section for various numerical correlations between $U_r$ and $E_\alpha$ determined by equation (1). For this purpose, we used the transmission coefficient calculation method which depends on $E_\alpha$ as well as on $U_r$, an approach which was proposed in reference [17].

A comparison of experimental alpha-particle emission spectra for the $^{60}$Ni(n,α) reaction at neutron energies of 9.4 MeV and 11 MeV, with theoretical spectra, which were calculated for different transmission coefficients, is shown in Figs. 6 and 7.

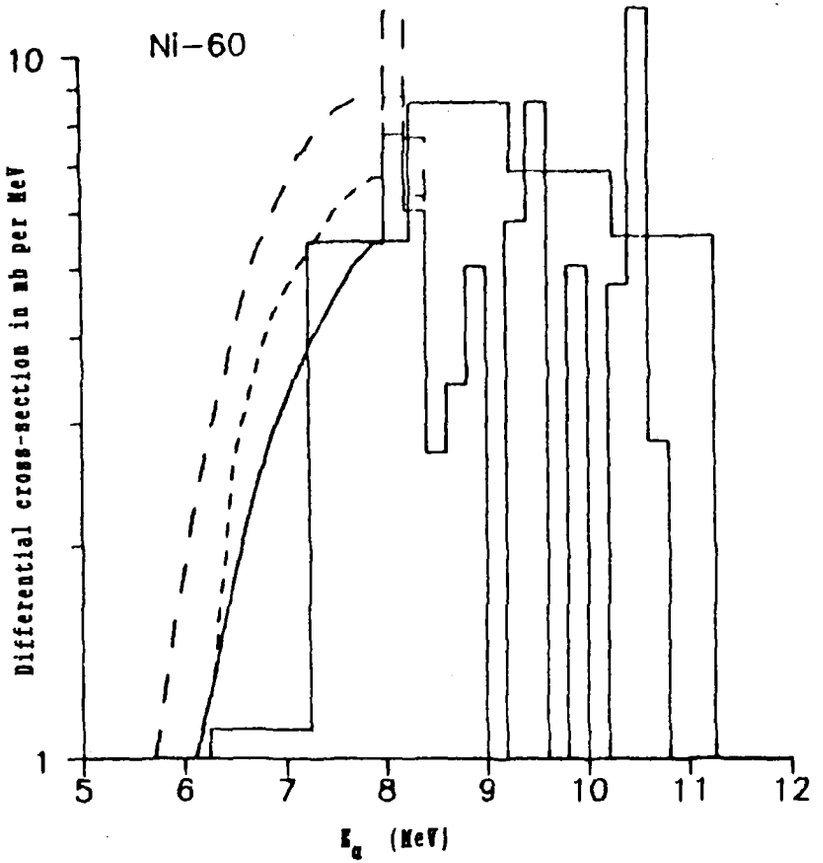


Fig. 6. Alpha-particle spectrum generated by the $^{60}Ni(n,\alpha)$ reaction at a neutron energy of $E_n$ = 9.4 MeV.

Experimental data: histogram [24].

Calculated curves:
Continuous curve - reference [16] potential;
Dashed curve - reference [15] potential;
Dotted curve - reference [16] potential.

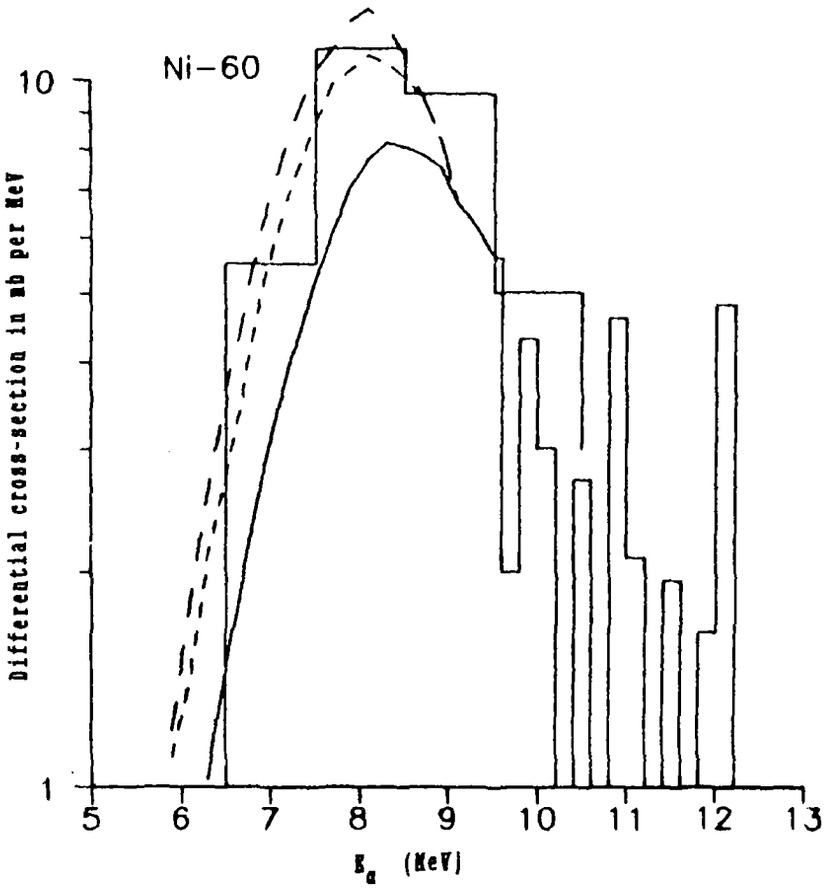


Fig. 7. Alpha-particle spectrum generated by the $^{60}Ni(n,\alpha)$ reaction at a neutron energy of $E_n$ = 12 MeV.

(Same caption designations as in Fi. 6.)

## Conclusion

This report consists of a discussion of the development and initial results of an evaluation of particle emission spectra generated by (n,p), (n,α), (n,2n), (n,n'p) and (n,n'α) neutron reactions for isotopes of chromium, iron and nickel. The evaluated data, presented in ENDF/B format at 1 MeV neutron energy intervals, between the threshold energy of the respective reactions and 20 MeV, have also been entered in the domestic evaluated data library BROND.

## REFERENCES


[1] YOUNG, P.G., "Application of nuclear models to neutron nuclear cross-section calculations" (Proc. Int. Conf. Nuclear Data for Science and Technology, Antwerp, 1982). (1983) 506.

[2] IGNATYUK, A.V., LUNEV, V.P., PRONYAEV, B.G., Izv. Akad. Nauk. SSSR, Ser.Fiz. 39 (1975) 2144 (in Russian).
FESHBACH, H., KERMAN, A., KOONIN, S., Ann. Phys., New York, 125 (1980) 429.

[3] KALBACH, C., Z.Phys., A 283 (1977) 401.

[4] GADIOLY, E., GADIOLY ERBA, E., HOGAN, J.J., Phys. Rev. C 16 (1977) 1404.

[5] RIBANSKY, I, OBLOZINSKY, P., Phys .Lett. B(NL) 45 (1973) 318.

[6] IWAMOTO, A., HARADA, K., Phys. Rev. C 26 (1982) 1821.

[7] BLOKHIN, A.I., IGNATYUK, A.V., PASHCHENKO, A.B., et al., Izv. Akad. Nauk. SSSR, Ser.Fiz. 49 (1985) 962 (in Russian)

[8] KALBACH, C., Nucl. Phys. A 210 (1973) 590.

[9] GRUDZEVICH, O.T., IGNATYUK, A.V., MANOKHIN, V.N., et al., in Proc. IAEA Res. Coord .Mtg., Bologna (1986) 61.

[10] ZELENETSKIJ, A.V., IGNATYUK, A.V., PASHCHENKO, A.B., Problems of Atomic Science and Technology, Ser. Nuclear Constants (1990) (in Russian).

[11] WILLIAMS, F.S., Nucl.Phys.A 166 (1971) 231.

[12] HAUSER, W., FESHBACH, H., The inelastic scattering of neutrons, Phys. Rev. 87 (1952) 366.
MOLDAUER, P.A., Statistical theory and nuclear collision cross-sections, Phys. Rev. B 135 (1964) 642.

[13] GRUDZEVICH, O.T., IGNATYUK, A.V., PLYASKIN, V.I., "Coordinated systematics of level densities for medium and heavy nuclei", in Proc. First Int. Conf. on Neutron Physics, Kiev, 1987. TsNIIatominform, Moscow, Vol.2 (1988) 96 (in Russian).

[14] HODGSON, P.E., Optical Model of Scattering, Atomizdat, Moscow (1966).

[15] BYCHKOV, V.M., ZELENETSKIJ, A.V., PASHCHENKO, A.B., in Proc. First Int. Conf. on Neutron Physics, Kiev, 1987. TsNIIatominform, Moscow, Vol.2 (1988) 102 (in Russian). BYCHKOV, V.M., GRUDZEVICH, O.T., ZELENETSKIJ, A.V., et al., "Absorption cross-sections of charged particles by nuclei in the ground and excited states", in Proc. Int. Conf. on Nuclear Data for Science and Technology, Mito, Japan, (1988) 1221.

[16] McFADDEN, L., SATCHLER, G.R., Nucl.Phys. 84 (1966) 177.

[17] ZELENETSKIJ, A.V., IGNATYUK, A.V., PASHCHENKO, A.B., Problems of Atomic Science and Technology. Ser. Nuclear Constants (1990) (in Russian).

[18] GRIMES, S.M., HAIGHT, R.C., ALVAR, K.R., et al., Phys. Rev. C 19 (1979) 2127.

[19] IGUCHI, A., TANAKA, S., AMANO, A., J. At. Soc. Jpn. 2 (1960) 682.

[20] VONACH, H., HAIGHT, R.C., WINKLER, G., Phys. Rev. C 28 (1983) 2278.

[21] TROBIK, W., et al., Phys. Rev. C 9 (1974) 5.

[22] HUYSINGA, I.R., IGO, G., Nucl. Phys. 29 (1962) 462.

[23] FISHER, R., TRAXLER, G., UHL, M., et al., Phys. Rev. C 30 (1984) 72.

[24] GRAHAM, S.L., AHMAD, M., GRIMES, S.M., Nucl. Sci. Eng. 95 (1987) 60.

# COMPARISON OF MEASURED AND CALCULATED CROSS-SECTIONS OF A LARGE NUMBER OF NUCLIDES

A.V. Zvonarev, V.A. Kolyzhenkov, V.G. Liforov,
G.N. Manturov, O.V. Matveev, I.M. Proshin,
Yu.S. Khomyakov, A.M. Tsibulya
Institute of Physics and Power Engineering, Obninsk

Abstract

The comparison of calculated and measured average cross-section ratios for a wide set of nuclides is presented. The cross-section reaction ratio data was measured over a period of thirty years on the fast neutron reactor BR-1. The experimental results are compared with calculations using different sets of neutron cross-sections.

A large amount of data on cross-section ratios has accumulated as a result of measurements performed on the fast reactor BR-1 [1] over the last thirty years. To satisfy the considerable interest to analyze this vast body of data with the objective to validate existing nuclear data and methods used in their calculation, an effort was undertaken to compile and process these data. The question arose in the process of this analysis on the comparability of the results obtained on different reactor configurations which had different compositions and geometries. The configuration of the BR-1-22 reactor assembly, which was built in 1978, has remained unchanged since then. The schematic of this configuration is shown on Fig. 1.

The basic difference between the last reactor assembly configuration and the earlier ones consisted in a different construction of the upper end reflector, an increase in the dimensions of the lower end reflector and of the core, as well as in the layout of the control mechanism with respect to the core. Reactor assemblies used in measurements prior to 1978 differed in the construction and composition of the side reflector as well as in the number of fuel elements in the core. Calculations showed that such alterations of the reactor configuration did not result in significant changes in the neutron spectrum in the central

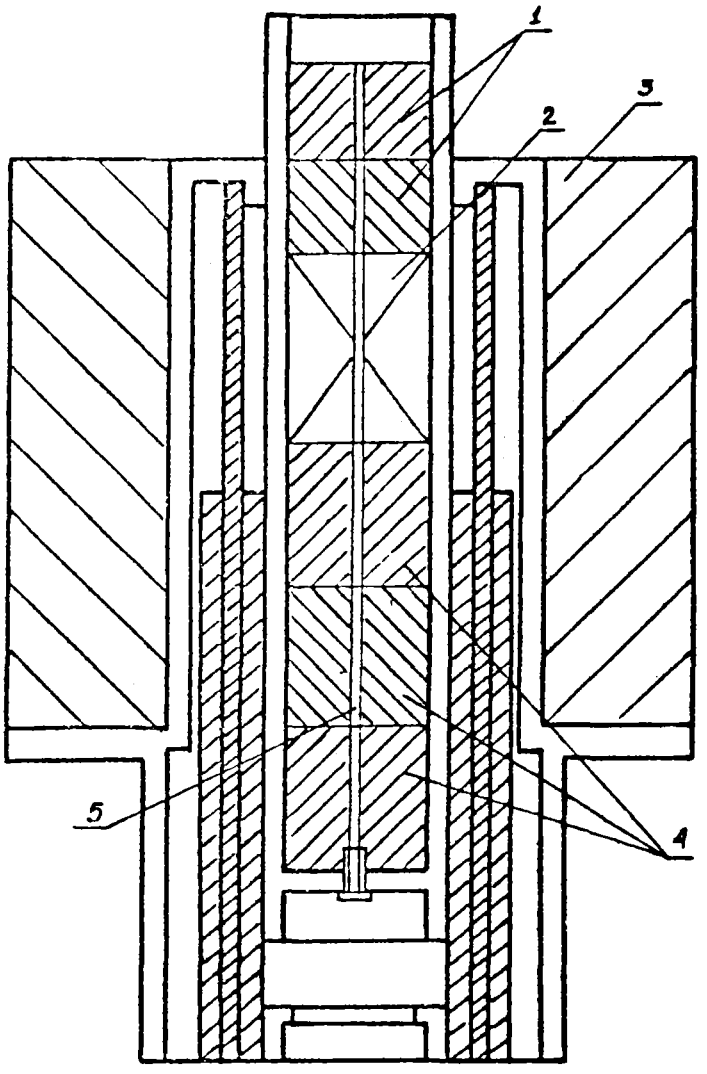


*FIG. 1. General schematic of the fast neutron BR-1 reactor (BR-1-22 assembly):*

*1 - upper end reflector*
*2 - reactor core*
*3 - side reflector*
*4 - lower end reflector*
*5 - experimental channel*

experimental channel of the reactor. The experimental results which were obtained on these earlier assemblies were adjusted to comply with the BR-1-22 reactor configuration; these calculated corrections of the measured data did not exceed 10%.

A comparison of the measured data has shown that the spread in the results was such that it was not possible to arrive at unequivocal conclusions for a number of reactions. As a result, it became evident that there was a need for a new set of measurements, especially since contemporary experimental methods

are so much better than the old ones. Consequently, it was decided to initiate a completely new cycle of measurements encompassing a much broader set of reactions. The first set of measurements on the BR-1 reactor consisted of a number of transactinium reaction cross-section measurements, providing data which are often used in the analysis of neutron spectra. These data gave us the possibility to analyze the neutron spectrum in the center of the BR-1 reactor, and to make more definitive conclusions regarding the quality of the group cross-section data used currently in reactor calculations. A few reaction cross-sections of structural materials were also measured.

## Description of the experiment

Most of the experimental information in this measurement cycle was obtained from measurements using activation detectors and a semiconductor gamma-ray spectrometer. Most detectors contained materials enriched in the isotope being measured. Using preliminarily calculated neutron reaction cross-sections of the isotopes being investigated, the weights of the samples were determined in such a way that the irradiation of all samples would create an approximately equal demand on the measurement procedure. After their weighing, the samples were enclosed in aluminium containers having a wall thickness of 0.2 mm. The samples were irradiated in the central experimental channel of the BR-1 reactor. A few samples were irradiated together simultaneously with uranium-235 samples for periods of time ranging from 1 to 10 hours in a fluence of $(2\text{-}20)\times10^{14}$ n/cm$^2$. The correction to compensate for the variation of the neutron flux with the position of the samples did not exceed 5%. This correction was determined from the results of a separate experiment which measured the response of the $^{235}$U(n,f) reaction along the axis of the experimental channel.

The measurements of the gamma ray spectrum of each sample was made in the same geometry with the aid of Ge(Li) detectors which had an effective sensitivity volume of 63 cm$^3$, and an energy resolution of 2.5 keV for $E_\gamma$=1332 keV. The data were recorded with an LP-4900 analyzer, and the spectra were processed with the

program PUCH on the SM-1420 computer. The following equation was used to determine the cross-section ratios:

$$\frac{\sigma^{i}(n,x)}{\sigma(n,f)} = \frac{A_i}{A_5}\,\frac{\varepsilon_5}{\varepsilon_i}\,\frac{\gamma_5}{\gamma_i}\,\frac{N_5}{N_i}\,\frac{K_5}{K_i}\,\frac{Y_5^m}{Y_i^m}\,\frac{\phi_5}{\phi_i}$$

where $A_i$ and $A_5$ - are the areas under the gamma ray peak, used to determine the response of the (n,x) reaction of the $i^{th}$ isotope and of the $^{235}U$ (n,f) reaction;

$\varepsilon_i$ and $\varepsilon_5$ - are the absolute efficiencies of the gamma ray detector;

$\gamma_i$ and $\gamma_5$ - are the absolute intensities of the measured gamma rays;

$N_i$ and $N_5$ - are the number of atoms of the $i^{th}$ isotope in the sample and in the uranium-235 sample;

$K_i$ and $K_5$ - are the gamma ray absorption coefficients of the sample material;

$Y_5^m$ and $Y_i^m$ - is the absolute value of the fission fragment yield, used here as the monitor for the $^{235}U$ (n,f) reaction; $Y_i^m=1$ for measurements of the (n,x) reaction response other than fission (i.e. $x\neq f$);

$\Phi_5/\Phi_i$ - is the ratio of the neutron flux at the $i^{th}$ isotope location to the flux at the $^{235}U$ sample location; and

T(t) - is a coefficient which takes into account the irradiation to cooling time ratio.

The OSGI-3M set of standard gamma ray sources was used to perform the efficiency calibration of the semiconductor gamma ray detector. The measured activities were corrected for the differences in the experimental geometries due to the different sample thicknesses and for the gamma ray absorption in the sample. Both corrections did not exceed 3%. The three fission fragments, $^{140}La$, $^{143}Se$, $^{97}Zr$, were used as monitors of the fission reaction. All other nuclear data needed for the processing of the experimental data were taken from references [2] an [3].

The measurement of the fission cross-section ratios of a number of isotopes was measured using solid-state track detectors (STD). The experimental set-up, which included the STD detector made of sodium silicate glass and a calibrated thin sample of the fissioning isotope, consisted of an aluminium cylinder and collimator positioned between the STD detector and the calibrated

sample. The calibrated samples of the fissioning isotopes, prepared at the V.G. Khlopin Radium Institute, were enriched to more than 99.9% in the measured isotope and had an uncertainty of 2% in the total number of atoms in the sample. The fission fragment tracks captured by the STD detector were identified after dissolving the detector glass in hydrofluoric acid to a point where the tracks were readily identified in a microscope with a 100-150 magnification. Track counting was done with an automatic scanning microscope. In order to increase the statistical accuracy, the counting was repeated 10-15 times. The counting was controlled periodically by a visual observation of the sample using a BIOLAM microscope. With the exception of one measurement, which will be described below, the new measurement results, which are in agreement with the data measured earlier, are listed in Tables 1 and 2.

**TABLE 1. RATIO OF REACTION CROSS-SECTION TO THE URANIUM-235 FISSION CROSS-SECTION FOR FISSILE NUCLIDES**

| Reaction | Experimental data | Calculation / Experiment |
|---|---|---|
| $^{232}$Th(n,f) | 0,0430 ± 0,0013 | 0,94±0,05 |
| $^{233}$U (n,f) | 1,54 ± 0,03 | 1,00±0,02 |
| $^{234}$U (n,f) | 0,790 ± 0,024 | 0,94±0,04 |
| $^{236}$U (n,f) | 0,333 ± 0,010 | 0,96±0,04 |
| $^{238}$U (n,f) | 0,165 ± 0,005 | 0,99±0,04 |
| $^{237}$Np(n,f) | 0,771 ± 0,023 | 1,04±0,04 |
| $^{239}$Pu(n,f) | 1,43 ± 0,04 | 0,94±0,03 |
| $^{240}$Pu(n,f) | 0,877 ± 0,026 | 0,91±0,03 |
| $^{241}$Pu(n,f) | 1,29 ± 0,04 | 1,02±0,03 |
| $^{242}$Pu(n,f) | 0,658 ± 0,020 | 0,98±0,03 |
| $^{241}$Am(n,f) | 0,825 ± 0,025 | 1,00±0,04 |
| $^{232}$Th(n,$\gamma$) | 0,109 ± 0,004 | 0,88±0,05 |
| $^{236}$U (n,$\gamma$) | 0,123 ± 0,006 | 0,87±0,07 |
| $^{238}$U (n,$\gamma$) | 0,077 ± 0,003 | 1,00±0,04 |
| $^{237}$Np(n,$\gamma$) | 0,240 ± 0,012 | 1,08±0,07 |
| $^{232}$Th(n,2n) | 0,00924±0,0005 | 1,07±0,08 |
| $^{238}$U (n,2n) | 0,00916±0,0005 | 0,97±0,08 |

TABLE 2. COMPARISON OF CALCULATED AND MEASURED RATIOS OF NEUTRON REACTION CROSS-SECTIONS TO THE URANIUM-235 FISSION CROSS-SECTION

| Reaction | Experimental data | Calculation / Experiment | Comment |
|---|---|---|---|
| $^{93}Nb\ (n,2n)^{92m}Nb$ | $(2,93\pm0,10)\ 10^{-4}$ | $2,61\pm0,06$ | |
| $^{27}Al\ (n,\alpha)\ ^{24}Na$ | $(4,3\pm0,2)\ 10^{-4}$ | $1,01\pm0,06$ | |
| $^{54}Fe\ (n,\alpha)\ ^{51}Cr$ | $(5,0\pm0,2)\ 10^{-4}$ | $0,71\pm0,05$ | |
| $^{59}Co\ (n,\alpha)\ ^{56}Mn$ | $(9,5\pm0,4)\ 10^{-4}$ | $1,02\pm0,06$ | |
| $^{92}Mo\ (n,\alpha)\ ^{89}Zr$ | $(5,5\pm0,5)\ 10^{-4}$ | $0,65\pm0,10$ | ENDF/B-V |
| $^{93}Nb\ (n,\alpha)\ ^{90m}Y$ | $(1,59\pm0,09)\ 10^{-5}$ | $2,23\pm0,07$ | ENDL-78 |
| $^{24}Mg\ (n,p)\ ^{24}Na$ | $(9,0\pm0,4)\ 10^{-4}$ | $0,84\pm0,06$ | |
| $^{27}Al\ (n,p)\ ^{27}Mg$ | $0,00221\pm0,00015$ | $0,95\pm0,08$ | |
| $^{46}Ti\ (n,p)\ ^{46}Sc$ | $0,0066\pm0,0003$ | $0,94\pm0,06$ | ENDF/B-V |
| $^{47}Ti\ (n,p)\ ^{47}Sc$ | $0,0097\pm0,0005$ | $1,24\pm0,06$ | ENDF/B-V |
| $^{48}Ti\ (n,p)\ ^{48}Sc$ | $(1,80\pm0,08)\ 10^{-4}$ | $0,93\pm0,06$ | ENDF/B-V |
| $^{54}Fe\ (n,p)\ ^{54}Mn$ | $0,0447\pm0,0015$ | $1,01\pm0,05$ | |
| $^{56}Fe\ (n,p)\ ^{56}Mn$ | $(6,1\pm0,2)\ 10^{-4}$ | $1,11\pm0,05$ | |
| $^{58}Ni\ (n,p)\ ^{58}Co$ | $0,055\pm0,003$ | $1,05\pm0,06$ | |
| $^{59}Co\ (n,p)\ ^{59}Fe$ | $(8,4\pm0,4)\ 10^{-4}$ | $0,87\pm0,06$ | |
| $^{92}Mo\ (n,p)\ ^{92m}Nb$ | $0,00388\pm0,00015$ | $0,51\pm0,05$ | ENDF/B-V |
| $^{50}Cr\ (n,\gamma)\ ^{51}Cr$ | $0,0057\pm0,0005$ | $0,61\pm0,09$ | |
| $^{55}Mn\ (n,\gamma)\ ^{56}Mn$ | $0,00297\pm0,00015$ | $1,20\pm0,05$ | |
| $^{58}Fe\ (n,\gamma)\ ^{59}Fe$ | $0,00228\pm0,00009$ | $1,46\pm0,05$ | |
| $^{59}Co\ (n\ \gamma)\ ^{60}Co$ | $0,0064\pm0,0003$ | $1,24\pm0,05$ | |
| $^{64}Ni\ (n,\gamma)\ ^{65}Ni$ | $0,00185\pm0,00008$ | $1,45\pm0,05$ | |
| $^{63}Cu\ (n,\gamma)\ ^{64}Cu$ | $0,0114\pm0,0005$ | $0,95\pm0,05$ | ENDF/B-V |
| $^{65}Cu\ (n,\gamma)\ ^{66}Cu$ | $0,0076\pm0,0006$ | $1,26\pm0,07$ | JENDL-2 |
| $^{98}Mo\ (n,\gamma)\ ^{99}Mo$ | $0,0193\pm0,0008$ | $1,48\pm0,04$ | |
| $^{94}Zr\ (n,\gamma)\ ^{95}Zr$ | $0,0064\pm0,0004$ | $1,15\pm0,06$ | JENDL-1 |
| $^{96}Zr\ (n,\gamma)\ ^{97}Zr$ | $0,00306\pm0,00015$ | $7,02\pm0,05$ | JENDL-1 |
| $^{115}In\ (n,n')^{115m}In$ | $0,102\pm0,006$ | $0,95\pm0,07$ | ENDF/B |
| $^{197}Au\ (n,\gamma)\ ^{198}Au$ | $0,105\pm0,005$ | $0,93\pm0,05$ | |

## Analysis of the experiment

The neutron spectrum in the center of the BR-1-22 assembly was calculated in a multi-group approximation with the three-dimensional MMKFK Monte-Carlo code [4], the two-dimensional DOT code and the one-dimensional KRAB-1 code using the ARAMOKO data processing system and the BNAB-78 multi-group constants [5]. The results of all three spectrum calculations were in good agreement. Calculations were also performed to study the effect of the central experimental channel on the neutron flux in the center of the assembly using the MMKFK and DOT codes. These calculations showed that there were no noticeable effects. Consequently, these results gave grounds for performing the analysis of the experiments in a one-dimensional geometry. The ratios of the average reaction cross-sections to the $^{235}U$ fission cross-section in the BR-1-22 spectrum were calculated with the BNAB-90 multi-group data file which was revised on the basis of new evaluated neutron data files [6]. Data from the BOSPOR-80 [7], ENDF/B-IV and -V, and JENDL-1 and -2 were also taken into account. The calculations of the simulated experiments which had been measured on earlier assemblies were performed in a one-dimensional geometry in an $S_{16}$ approximation. Calculations were also performed to determine the ratios of the spectral indexes in the center of these earlier assemblies to the values of these indexes calculated for the BR-1-22 assembly. As mentioned above, the results of experiments performed on these earlier assemblies were "converted" to the BR-1-22 assembly characteristics with the aid of these ratios.

An evaluation of the errors in the calculation of the group neutron spectra and of the average reaction cross-sections was performed in order to insure the correctness of the results of the subsequent analysis of the experiment simulation. The matrix for the group neutron flux errors caused by the uncertainties in the values of the multi-group constants was calculated with the following formula:

$$V_\varphi = H W_\sigma H^T$$

where $W_\sigma$ is the covariance matrix of the group cross-section errors [5], and H is the matrix of the sensitivities of the group spectra to the cross-sections.

The covariance matrix of the errors resulting from the calculation of the average cross-sections is composed of two matrices: the first describes the errors which arise as a result of uncertainties in the group flux values, and the second results from the uncertainties in the values of the reaction cross-sections. The error matrix of the group spectrum values $V_\phi$ must also include the systematic component of the calculational error. The evaluation of this component of the error can be made by comparing the results of calculations of experimental simulations in various geometries using different methods to solve the transport equation performed with the MMKFK, DOT and KRAB-1 codes. In view of the good agreement in the results of such calculations (the differences in the values of group spectra did not exceed 3%) it can be concluded that this error component is small, and in any case considerably smaller than that of the group constants.

This analysis showed the following:

1. The divergence between calculation and experiment for threshold reactions has an expected dependence, which grows with the increase of the reaction threshold. This is illustrated in Fig. 2, which shows the ratios of calculated to measured values of a number of reaction cross-sections as a function of the parameter $G_i$, which can be considered as the average for the group:

$$G_i = \frac{\sum_g g\,\sigma_i^g \phi^g}{\sum_g \sigma_i^g \phi^g}$$

where i is the number of the reaction.

2. For many reactions, the error of the calculated average cross-section, which is dependent on the error of the calculated spectrum, is substantial (exceeding the experimental error by a factor of 2 to 3 for some reactions). This means that in order to be able to utilize the obtained experimental information in the analysis of measured reaction cross-sections, it is essential to correct and improve the accuracy of the neutron spectrum. This was done in the processing of experimental data for 16

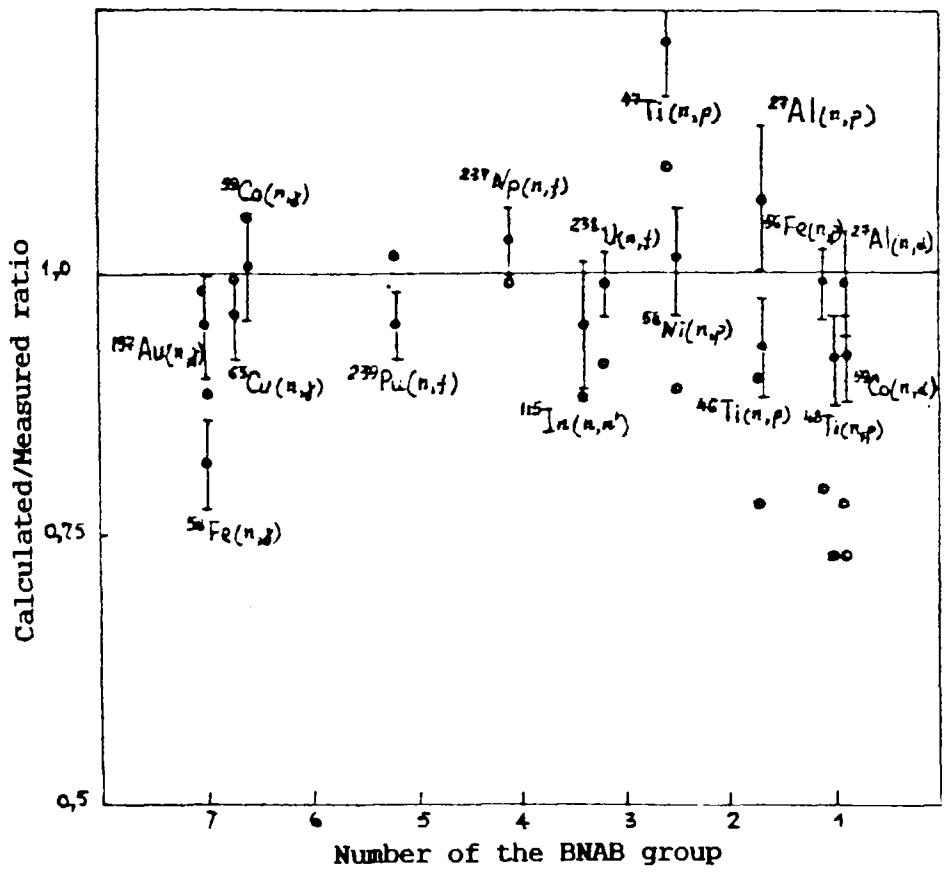


*FIG. 2. Ratio of calculated to measured data for sixteen reactions calculated for two different neutron spectra:*

*∘ - spectrum calculated with the KRAB-1 code*
*• - corrected spectrum*

reactions. Reaction data were selected for the correction of the calculated spectrum using the following criteria: a) that the chosen sensitivity ranges cover the full energy range of the neutron spectrum of the BR-1 reactor, b) that the information on the cross-sections for the given reactions is reliable (we used the ENDF/B-V dosimetry file), and most important, c) that these reaction cross-sections included their uncertainties [8]. Using the least-squares method for the correction procedure, the best way to evaluate the spectrum is by using the available experimental data, and the best way to evaluate its accuracy is by using the information on the cross-section uncertainties. This is the procedure that was adopted. The corrected neutron spectrum in the center of the BR-1-22 assembly is given in Table 3, and Fig. 2 shows the calculated to measured ratios for the data of 16 reactions after the correction of the neutron spectrum

TABLE 3. GROUP NEUTRON SPECTRUM IN THE BR-1 REACTOR CENTER

| g | Calculated Spectrum | Corrected Spectrum | Spectrum error after correction % |
|---|---|---|---|
| -1 | $1,0 * 10^{-5}$ | $1,6 * 10^{-5}$ | 10 |
| 0 | $5,0 * 10^{-4}$ | $6,97 * 10^{-4}$ | 6 |
| 1 | 0,0110 | 0,0137 | 4 |
| 2 | 0,0554 | 0,0636 | 3 |
| 3 | 0,1129 | 0,1254 | 3 |
| 4 | 0,1770 | 0,1794 | 3 |
| 5 | 0,1650 | 0,1614 | 4 |
| 6 | 0,1908 | 0,1856 | 4 |
| 7 | 0,1430 | 0,1370 | 4 |
| 8 | 0,0834 | 0,0787 | 6 |
| 9 | 0,0419 | 0,0387 | 7 |
| 10 | 0,0139 | 0,0118 | 8 |
| 11 | 0,00490 | 0,0038 | 12 |
| 12 | $2,79 * 10^{-4}$ | $2,15 * 10^{-4}$ | 15 |

**Annotation: the upper energy boundary of the first group is taken to be 20 MeV (in the BNAB system it is equal to 14.5 MeV)**

had been taken into account. The data listed in Table 3 shows that the corrected spectrum diverges considerably from the calculated spectrum in the upper energy region of the spectrum (i.e., groups -1 to 3). These differences can be attributed most probably to the uncertainties assigned to the elastic scattering cross-section and to the fission neutron spectrum of $^{239}Pu$. The differences between the calculated and the experimental data were finally determined on the basis of the corrected spectrum; these differences are listed in Tables 1 and 2. Except where indicated, the BNAB-90 set of evaluated reaction cross-section data was used in these calculations. It should be noted that the uncertainties given in Tables 1 and 2 include the experimental error and the compound spectral error used in the calculation of the average cross-sections. Consequently, should the differences in the data be larger than the limits of the given uncertainties, the reason for this should be sought in the first place in the values of the reaction cross-sections.

## Analysis of the results

The data in Table 1 shows that there is good agreement between the calculated and measured transactinium reaction cross-sections. The following should be noted.

- The experimentally determined $^{240}$Pu fission cross-section exceeds the calculated value by 9%, which is equivalent to three times the experimental error.

- The value of the average $^{236}$U capture cross-section was calculated using the results of its last evaluation based on the data reported in reference [9]; calculational results which were based on earlier evaluations (e.g. ENDF/B-V) are approximately 45% higher than the measured value.

- The difference between the calculated and measured values of the $^{239}$Pu fission cross-sections does not exceed two times the value of the experimental error; however, it must be noted that the ratio of the cross-section of this reaction to the $^{235}$U fission cross-section, obtained on the basis of the latest experiments, differs by 8% from results obtained earlier. This difference between calculation and experiment for reactions included in Table 2 is more substantial than for those listed in Table 1.

In addition, the following comments can be made:

- The calculation of the average $^{93}$Nb (n,2n) and (n,$\alpha$) reaction cross-sections were made using evaluated partial reaction cross-sections. As shown by the experimental results reported in reference [10], the reaction cross-sections (leading to the formation of the $^{92m}$Nb and the $^{90m}$Y metastable states which have been measured in this experiment), are significantly lower and do not contradict the experimental results obtained on the BR-1 reactor.

- Reference [10] lists the latest experimental data on the microscopic $^{92}$Mo (n,p) and (n,$\alpha$) reaction cross-sections. These results, which have been included in the ENDF/B-V evaluation, point to lower values which do not contradict the results obtained on the BR-1 reactor.

- A similar situation has been observed in the case of the $^{96}$Zr capture reaction. The experimental data given in reference

TABLE 4. RATIO OF CALCULATED TO MEASURED DATA FOR THE RATIO OF DIFFERENT REACTION CROSS-SECTIONS TO THE URANIUM-235 FISSION CROSS-SECTION CALCULATED FOR DATA FROM DIFFERENT EVALUATED DATA LIBRARIES

| Reaction | BNAB-90 | ENDF/B | JENDL | BOSPOR |
|---|---|---|---|---|
| $^{24}Mg(n,p)$ | 0,84 | - | - | 1,05 |
| $^{27}Al(n,p)$ | 0,95 | 1,08 | 2,91 | 1,05 |
| $^{27}Al(n,\alpha)$ | 1,01 | 1,00 | 0,99 | 1,01 |
| $^{46}Ti(n,p)$ | - | 0,94 | - | 1,11 |
| $^{47}Ti(n,p)$ | - | 1,24 | - | 1,26 |
| $^{48}Ti(n,p)$ | - | 0,93 | - | 0,90 |
| $^{50}Cr(n,\gamma)$ | 0,61 | - | 1,14 | - |
| $^{54}Fe(n,p)$ | 1,02 | - | 0,95 | 1,02 |
| $^{54}Fe(n,\alpha)$ | 0,71 | - | 1,49 | 0,74 |
| $^{55}Mn(n,\gamma)$ | 1,20 | 1,53*) | 1,26 | - |
| $^{56}Fe(n,p)$ | 1,12 | 0,99 | 1,13 | 1,08 |
| $^{58}Ni(n,p)$ | 1,05 | 1,02 | 1,01 | 1,03 |
| $^{58}Fe(n,\gamma)$ | 1,46 | 0,81 | 0,58 | - |
| $^{59}Co(n,\gamma)$ | 1,24 | 1,01 | 0,57 | - |
| $^{59}Co(n,\alpha)$ | 1,02 | 0,93 | 0,95 | 0,95 |
| $^{59}Co(n,p)$ | 0,88 | 1,85*) | 1,85*) | 0,79 |
| $^{63}Cu(n,\gamma)$ | - | 0,95 | 1,73 | - |

*) calculated on the basis of ENDF/B data

[10], which shows a significant increase in the value of the cross-section, have been included in the JENDL-1 evaluation.

- The ratios of calculated data, which were derived from cross-sections taken from different data libraries, to the experimentally determined data are listed in Table 4. This comparison shows that there are rather large differences between the data from various data libraries.

This analysis shows that the experimental results obtained in this work do not contradict current data on microscopic cross-sections, and can be effectively used in the testing and the further refinement of the data.

## REFERENCES


[1] LEIPUNSKIJ, A.I., ABRAMOV, A.I., ANDREEV, V.I., et al., Fast neutron reactor physics, At. Ehnerg. 5 (1958) 277-292 (in Russian).

[2] RYDER, B., MEEK, M., Compilation of fision product yields, Rep. NEDO-12154-3(B) (1980).

[3] Nuclear Data Sheets, Academic Press, New York.

[4] KAZAKOVA, L.B., KAMAEVA, O.B., KOROBEINIKOVA, L.B., et al., Monte Carlo Methods in Mathematical Computations and Mathematical Physics, SO Akad. Nauk SSSR, Novosibirsk (1985) 114-121 (in Russian).

[5] ABAGYAN,l.P., BAZAZYANTS, N.O., NIKOLAEV, M.N., TSIBULYA, A.M., Group Constants for Reactor and Shielding Calculations, Ehnergoizdat, Moscow (1981) (in Russian).

[6] KOSHCHEEV, V.N., NIKOLAEV, M.N., Problems in Atomic Science and Technology, Ser. Nuclear Constants 5(59) (1984) 16 (in Russian).

[7] BYCHKOV, V.M., ZOLOTAREV, K.N., PASHCHENKO, A.B., PLYASKIN, V.N., Problems in Atomic Science and Technology, Ser. 3(42) (1981) 60 (in Russian).

[8] NOLTHENIUS, H.J., ZIJP, W.L., (Proc. IAEA Cons. Mtg. on Nuclear Data for Radiation Damage Estimates for Reactor Structural Materials, Santa Fe, NM, 1985) Rep. INDC(NDS)-179, IAEA, Vienna (1986).

[9] MACKLIN, R.L., ALEXANDER, C.W., Neutron absorption cross-section of uranium-236, Rep. ORNL/TM-10999 (1988).

[10] MCLANE, V., Neutron Cross-Sections, Academic Press, New York, Vol.2 (1988).